

8-2008

The Mayan Ice Cap: Glacial Geology and Paleoclimate of the Northern Guatemalan Highlands

Alex Joseph Roy
University of Nevada, Las Vegas

Follow this and additional works at: <https://digitalscholarship.unlv.edu/thesesdissertations>



Part of the [Climate Commons](#), [Geology Commons](#), and the [Glaciology Commons](#)

Repository Citation

Roy, Alex Joseph, "The Mayan Ice Cap: Glacial Geology and Paleoclimate of the Northern Guatemalan Highlands" (2008). *UNLV Theses, Dissertations, Professional Papers, and Capstones*. 1078.
<https://digitalscholarship.unlv.edu/thesesdissertations/1078>

This Thesis is protected by copyright and/or related rights. It has been brought to you by Digital Scholarship@UNLV with permission from the rights-holder(s). You are free to use this Thesis in any way that is permitted by the copyright and related rights legislation that applies to your use. For other uses you need to obtain permission from the rights-holder(s) directly, unless additional rights are indicated by a Creative Commons license in the record and/or on the work itself.

This Thesis has been accepted for inclusion in UNLV Theses, Dissertations, Professional Papers, and Capstones by an authorized administrator of Digital Scholarship@UNLV. For more information, please contact digitalscholarship@unlv.edu.

THE MAYAN ICE CAP: GLACIAL GEOLOGY AND
PALEOCLIMATE OF THE NORTHERN
GUATEMALAN HIGHLANDS

by

Alex Joseph Roy

Bachelor of Science
University of Maine, Orono
2005

A thesis submitted in partial fulfillment
of the requirements for the

**Master of Sciences Degree in Geoscience
Department of Geosciences
College of Sciences**

**Graduate College
University of Nevada, Las Vegas
August 2008**

ABSTRACT

The Mayan Ice Cap: Glacial Geology and Paleoclimate of the Northern Guatemalan Highlands

by

Alex Joseph Roy

Dr. Matthew Lachniet, Examination Committee Chair
Assistant Professor of Geology
University of Nevada, Las Vegas

The Sierra de los Cuchumatanes region of the northern Guatemalan highlands supported a large plateau ice cap with an area of ~40 km² along with a group of 5 cirque glaciers ~1 to 2 km² during the local last glacial maximum (LLGM). A comprehensive mapping reconstruction of the northern Guatemalan highlands is presented here, including glacial geology and an estimate of maximum ice limits from physical evidence and computer modeling. The glacial geologic map was produced via field mapping with global positioning system (GPS) surveying combined with aerial stereo photographic and topographic map analysis. This new field work on moraine limits expands upon previous reconnaissance-level studies and preliminary reconstruction efforts. Elevation of the northern Guatemalan highlands LLGM_{BR=2.0} equilibrium line altitude (ELA) was estimated to be 3515 m for the cirque glaciers and an average of 3703 m for the plateau ice cap. Glacial evidence and regional climate data were employed as input to a physically based geographical information system (GIS) mass-balance model, developed by Plummer and Phillips (2003). Using the target ELA of the ice cap (3650 m) and cirque

(3550 m) glaciers, the mass balance model results reveal that an average LLGM temperature depression was -5.0°C from present day, accompanied by precipitation that was equal to 100% of present day totals. Using the present day Central American ELA of 4900 ± 200 m, the glacial evidence shows 1197 ± 200 m of ELA lowering for the plateau ice cap and 1385 ± 200 m for the north facing cirques. When the amount of ELA lowering is multiplied by the Guatemalan temperature lapse rate of $-5.3^{\circ}\text{C km}^{-1}$, an LLGM cooling is given as $-7.4 \pm 1.1^{\circ}\text{C}$ for the cirques and a $-6.4 \pm 1.1^{\circ}\text{C}$ average for the plateau ice cap. Although the physical evidence suggests a greater temperature reduction, during the LLGM of Guatemala, than the GIS model output, both methods place detailed constraints on Guatemalan highland paleoclimate and the LLGM ELA. Although the age of the Guatemalan glacial maximum is unconstrained, a qualitative assessment of moraine morphology suggests a correlation between the plateau moraines and the LLGM (20 to 17.5 ka) moraines of Mexico.

TABLE OF CONTENTS

ABSTRACT.....	iii
LIST OF FIGURES	vii
LIST OF TABLES	viii
ACKNOWLEDGEMENTS.....	ix
CHAPTER 1 INTRODUCTION	1
Geology of Guatemala	4
Modern Climate of Guatemala.....	5
Regional Late Quaternary climate	9
Estimating the equilibrium line altitude (ELA)	13
Central American Late Quaternary ELAs.....	16
CHAPTER 2 METHODS	19
Glacial Geology	19
Building the GIS	23
Glacier Modeling	26
THAR, AAR, AABR and Ice Thickness	30
CHAPTER 3 RESULTS	33
Glacial Geomorphology.....	33
Ice cap and cirque glaciers.....	36
Past and Present ELAs	40
Glacier modeling estimates.....	43
CHAPTER 4 DISCUSSION.....	51
The Mayan Ice cap and cirque glaciers.....	51
Paleotemperature Discrepancies	53
Highland Glacier Dynamics.....	55
Future Work.....	58
REFERENCES	61
APPENDIX I GIS MODEL CLIMATE DATA	67
APPENDIX II GUATEMALAN TEMPERATURE AND PRECIPITATION	72

APPENDIX III	EXAMPLES OF MASS BALANCE MODEL OUTPUT.....	76
VITA.....		81

LIST OF FIGURES

Figure 1	Generalized location map of Central America	2
Figure 2	A 500m digital elevation model (DEM) of Guatemala	6
Figure 3	A topographic map of the Sierra de los Cuchumatanes region.	7
Figure 4	A map-view diagram of the accumulation and ablation areas	15
Figure 5	A small whaleback in the eastern Ninguitz Valley	20
Figure 6	A large lateral moraine of the Ninguitz Valley	21
Figure 7	Deposit of large boulder sized till material	22
Figure 8	Aerial photograph of the western Colinas Planas region.	24
Figure 9	Methods employed to create the final glacial geologic map	25
Figure 10	A plot of the average annual temperature vs. station elevation.....	28
Figure 11	Glacial geologic map of the plateau region and Montaña San Juan.....	34
Figure 12	Map of the reconstructed Mayan ice cap.....	37
Figure 13	Map of the reconstructed cirque glaciers.....	39
Figure 14	Climate-space diagram	46
Figure 15	A plot of mass balance gradients for the reconstructed cirque glaciers.	47
Figure 16	One version of the modeled maximum ice extent	49
Figure 17	Topographic profile of the plateau region and Montaña San Juan.....	55
Figure 18	DEM showing the location of ephemeral moraine dammed lakes.....	58

LIST OF TABLES

Table 1	Climate input for the mass balance GIS model	27
Table 2	Equilibrium line altitude (ELA) estimates from the glacial evidence	41
Table 3	Estimates of the Δ ELA from glacial evidence.....	41
Table 4	Estimates of temperature depression from glacial evidence.....	43
Table 5	GIS modeled LLGM paleoclimate and ELAs	45

ACKNOWLEDGEMENTS

My academic endeavors could not have been possible without the continuous encouragement and tireless support of one person, Kristen L. Wood. I would like to thank my graduate advisor, Matthew S. Lachniet for his unending enthusiasm for all things glacial, and his patience and outlook while working together on this project. I would like to thank my committee members Terry Spell, Andrew Hanson and John Swetnam for their guidance in strengthening my thesis, and their positive attitude and comments. Conversations with several individuals also contributed to the evolution of this project; Mitch Plummer of the Idaho National Laboratory for allowing me to visit INL and the endless instruction on his GIS model, Lorenzo Vázquez-Selem of the Universidad Nacional Autónoma de México, Mexico City for the relative chronology and Rebecca Huntoon of UNLV Geoscience for her assistance with GIS difficulties.

Funding for this research came from the UNLV Geoscience scholarships Bernada E. French funds and the UNLV Graduate and Professional Student Association Grant.

Finally I would like to thank April Azouz, Lael Vetter, Thomas Muntean, Paul Kosmidis and other graduate students who contributed scholastic support and extensive scientific discussion. Thanks to Pasquale Del Vecchio and other inspired Geomorphology students for enjoyable semester classes, along with UNLV Geoscience faculty, staff and students who have assisted my academic career. I would like to distinguish all the members of the Roy, O'Brien, Lombardi, Wood, Taylor and Cain families; my adventures would have never been realized without their unwavering support.

CHAPTER 1

INTRODUCTION

Glacial evidence found in highland areas provide an excellent record of climatic changes, especially changes in glacier mass balance due to temperature and precipitation fluctuations (Laabs et al., 2006; Benn and Lehmkuhl, 2000; Hostetler and Clark, 2000). In tropical highlands, glacial evidence may be the principal source of data for paleoclimate reconstruction (Hostetler and Clark, 2000) and comprehensive studies of Central American glaciated regions are limited to only a few viable locations (i.e., Guatemala, Costa Rica). The formerly glaciated Sierra de los Cuchumatanes of the northern Guatemalan highlands presents a unique opportunity to study Central American paleoclimate using glacial geomorphology and to complement previous work from nearby highlands in Costa Rica, Mexico and Venezuela (Fig. 1).

A recurring theme in recent tropical paleoclimatology is the inconsistency between the temperature estimates of the land surface and sea surface during the global last glacial maximum, called the ‘tropical temperature paradox’ (Seltzer, 1992; Porter, 2001; Mark et al., 2005; Lachniet and Vazquez-Selem, 2005). Estimates of Late Quaternary tropical sea surface temperatures (i.e. CLIMAP, 1976, 1981) were shown by Rind and Peteet (1985) to be less depressed than concurrent land surface temperatures during the global last glacial maximum. Tropical land surface temperature depressions for the Late Quaternary

range 5 to 8°C from present while concurrent sea surface temperature depressions are only estimated to ~2 to 3°C; not enough sea surface cooling to support data from tropical glacial records (Mark et al., 2005). The paleoclimate estimates from the northern Guatemala highlands, which are based on physical evidence and glacier modeling, will provide a more thorough tropical highland input for global climate model simulations.

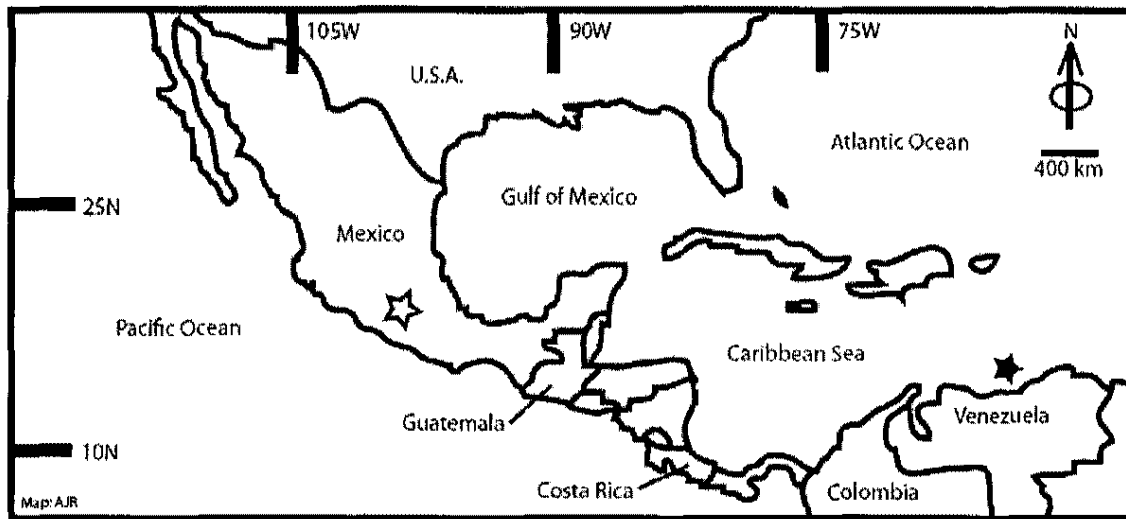


Figure 1. Generalized location map of Central America and surrounding regions. Open star represents the location of the Trans-Mexican volcanic belt (TMVB) and closed star shows the location of the Cariaco Basin, a large source of paleoclimatic proxy data for this region.

Interpreting formerly glaciated terrains provide an excellent scientific resource for constructing paleoclimate proxy records from glacier mass balance models (i.e., Benn and Lehmkuhl, 2000; Hostetler and Clark, 2000) and direct glacial evidence ice reconstructions (i.e., Lachniet and Seltzer, 2002). Assembling a record of paleo-temperature and paleo-precipitation values for tropical regions typically relies on a

variety of proxy records such as palynology and analysis of high mountain glacial ice core chemistry. In Guatemalan paleoclimate research the focus has been primarily on data obtained from sedimentary records cored in Lake Quexil, Guatemala (i.e., Leyden et al., 1994; Leyden, 2002) and the deepest lowland Central American Lake, Lake Petén Itzá, Guatemala (Anselmetti et al., 2006; Hodell et al., 2007; Hodell et al., 2008) located in the northern Guatemalan Lowlands (~15 m above sea level – a.s.l.) (Fig 2). These data provide a background for estimating the paleoclimate and moisture potential for the northern Guatemalan highlands, although location specific glacial evidence will allow a more realistic estimate of highland paleoclimate to be completed.

The primary focus of this research was to utilize the glacial geomorphology of the Sierra de los Cuchumatanes, including lateral, terminal and recessional moraine traces, scoured bedrock surfaces, outwash plains, ephemeral moraine dammed lake beds and other glacial landforms to reconstruct the greatest extent of ice in this region. From that reconstruction, an estimate of the regional temperature depression from present could be made. Mapping the physical remnants of the largest ice extent provided input for a physically based GIS mass balance glacier model by Plummer and Phillips (2003). The use of GIS-based studies in glacial geomorphology provide a computer-aided approach for reconstructing ice margins and interpreting complex glacial geomorphology where no glacier ice currently exists (Napieralski et al., 2007). The GIS model incorporates Guatemalan present-day climate data such as precipitation, temperature, cloudiness, wind-speed, along with estimated temperature and precipitation lapse rates, to estimate the climate that would be necessary to sustain steady-state glacier ice in this highland tropical environment.

Geology of Guatemala

According to Marshall (2006) few regions on the planet exhibit the geomorphic diversity of Central America, its structure defined principally by the northwest trending Middle America trench and the Central American volcanic province. Guatemala is the most northern country in Central America, located between $\sim 14^{\circ}$ to 18° N latitude, and is transected east to west by the large Polochic – Motagua - Chamalecon fault system which trends from the northeast to southwest (Fig. 2). These faults demarcate a continental boundary between the North American (Mayan block) and Caribbean plates (Chortis block) (Bundschuh and Alvarado, 2007) along with dominating the varied topography of Guatemala.

The Mayan block is topped by a thick sequence of upper-Paleozoic clastic and carbonate sediments, along with Cretaceous to Eocene carbonate and evaporate rocks (Bundschuh and Alvarado, 2007). The study area (Fig. 3) is centered atop the highest portion of the Sierra de los Cuchumatanes, a northwest trending extension of Mexico's Sierra Madre Massif, which is located within the Mayan Highlands section of northern Central America. The Sierra de los Cuchumatanes is formed primarily upon a ~ 2500 m thick sequence of Cretaceous Limestone and Dolomite extensively capping the Mayan highlands sedimentary sequence (Bundschuh and Alvarado, 2007). This limestone plateau which rests primarily on the Mayan Block corresponds to the most southern limit of the North American continent, and contains the highest non-volcanic point in Central America at 3837 m.

Modern Climate of Guatemala

The present day Guatemalan climate is influenced locally by the varied topography but regionally by its proximity to the Gulf of Mexico, Caribbean Sea and Pacific Ocean. The average monthly precipitation cycle for the northern Guatemalan highlands consists of a pronounced summer wet season starting in April and ending mid-September. The wet season is punctuated by drier winter conditions between October and March, along with a slight precipitation minimum during the mid-summer wet season centered on mid-July. Mean annual temperature for Todos Santos Cuchumatán (2480 m), a small town located west of the main field area (Fig. 3), is $\sim 14.2^{\circ}\text{C}$ with a mean annual precipitation total of ~ 1155 mm ($n = 15\text{y}$). Data for relative humidity, cloud cover and number of days with rain indicates that the climate of Todos Santos is humid inner-tropical with a mean annual humidity of $\sim 84.1\%$. Since there are no direct climate measurements at the field area (i.e., plateau), present day precipitation and temperature is estimated from the present day atmospheric lapse rate of $-5.3^{\circ}\text{C km}^{-1}$, which measures the change in temperature with rising altitude, and average annual temperature of Todos Santos (14.2°C) giving an annual average temperature on the main plateau at ~ 3700 m to be $\sim 7.7^{\circ}\text{C}$. The current atmospheric temperature lapse rate was calculated by comparing the monthly average temperature data of a lowland station in Puerto San Jose to the highland town of Todos Santos, which was later confirmed by comparing averages for multiple stations throughout Guatemala. Isohyet maps for Guatemalan precipitation and isotherm maps for temperature (INSIVUMEH, 2006) show that the eastern regions near the Caribbean Sea, along with the windward Pacific facing highlands have higher

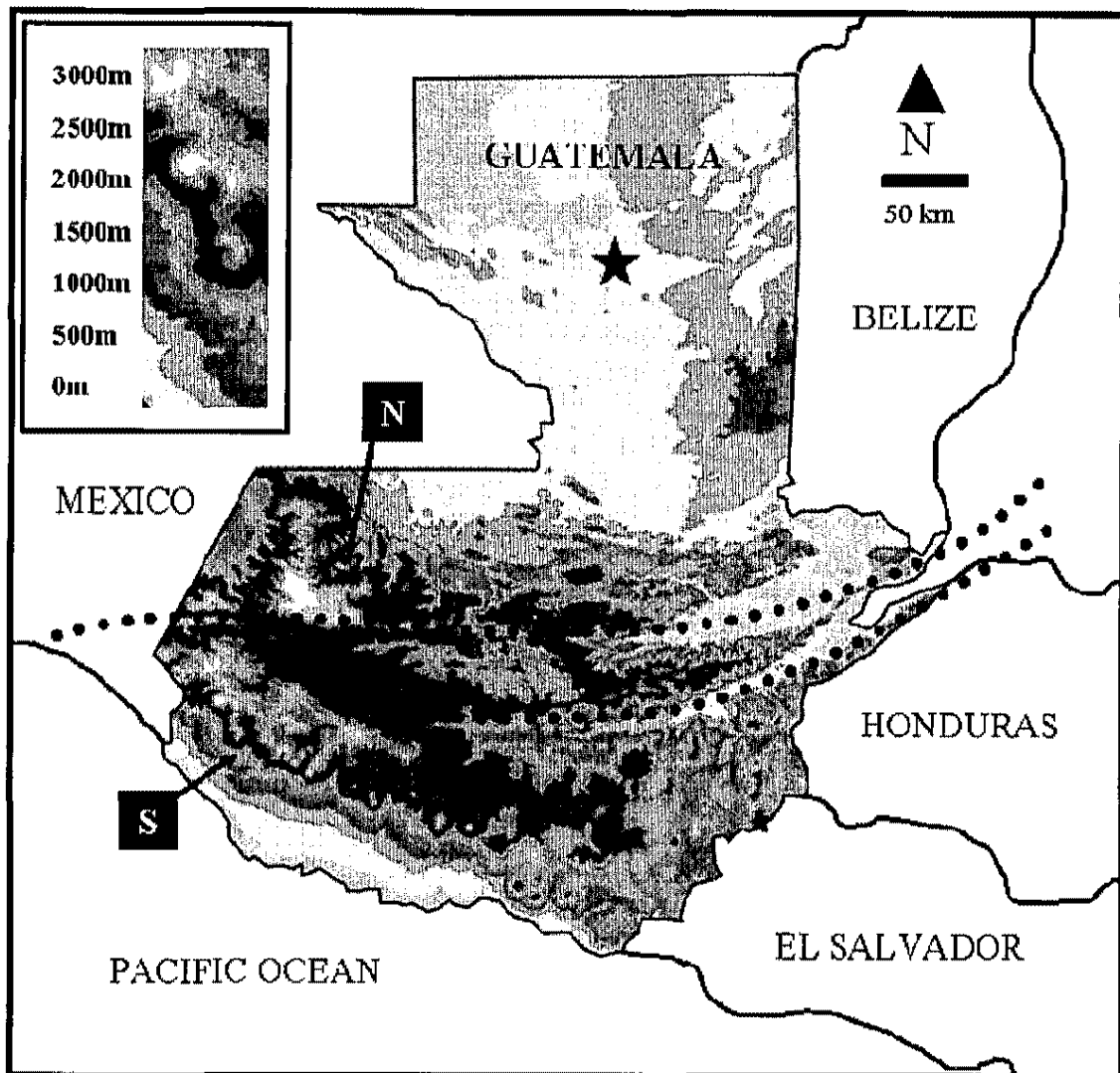


Figure 2. A 500m digital elevation model (DEM) of Guatemala along with bordering Central American countries. Dotted lines are large transform faults which demarcate the North American and Caribbean tectonic plates. The northern highlands (N) contain the Sierra de los Cuchumatanes region and the field area (centered on 91.5°W ; 15.5°N) while the southern highland (S) consists of volcanic peaks from the Central American Volcanic province. Black star in the northern lowlands represents the location of Lake Petén Itzá and Lake Quexil mentioned in the text.

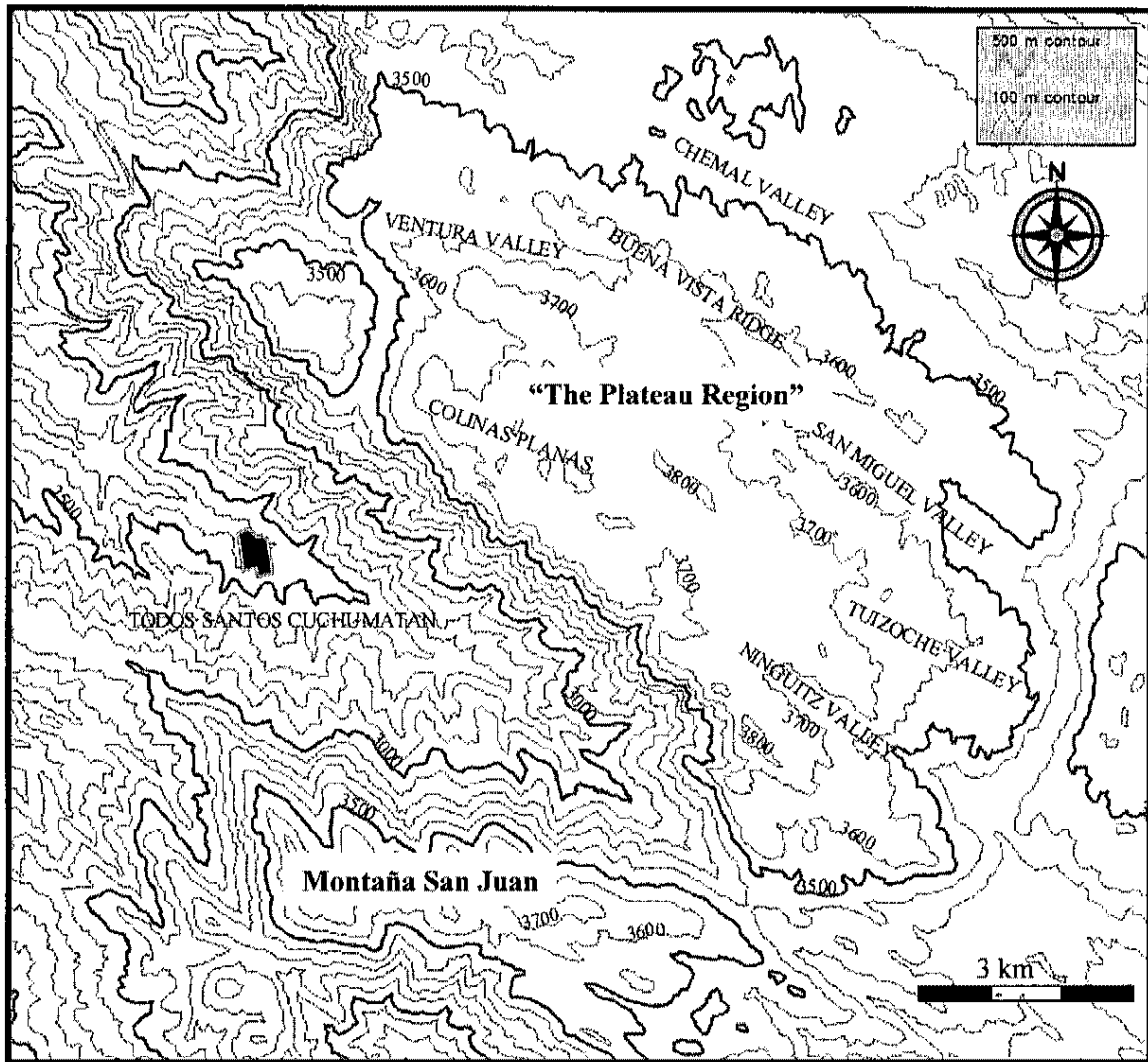


Figure 3. A topographic map of the Sierra de los Cuchumatanes region located in the northern Guatemalan highlands, including the plateau region and Montaña San Juan. The town of Todos Santos Cuchumatán is shown, along with the specific valley names and locations mentioned in the text; the San Miguel Valley is centered on $\sim 91.5^{\circ}\text{W}$, 15.5°N .

precipitation maximums suggesting some orographic precipitation influences of the southern highlands and precipitation increases due to the easterly trade winds. Similarly the interior regions of Guatemala, including the field area, show dramatic decreases in precipitation compared to other more coastal sites on the Caribbean Sea at the same latitude (INSIVUMEH, 2006).

Based on 30 years of Central American climate observations, Portig (1965) reported that the primary wind directions during the dry winter months (December, January, February) are predominately from the NNE to NE while summer (June, July, August) winds, associated with increased easterlies and the inter-tropical convergence zone (ITCZ), are from the ESE. An increase in trade wind strength combined with orographic uplift produces a precipitation maximum on the Caribbean and inland along the Pacific coast. In a region dominated by easterly trade winds such as Central America, an increase in sea surface temperatures in the eastern Atlantic or Caribbean Sea could effect orographic precipitation, partially due to increased evaporation in the Caribbean Sea or Gulf of Mexico along with increasing the duration of the tropical cyclone season (Aguilar et al., 2005). Pacific sources also play an important role in contributing to the precipitation that reaches Central America, including the slight depression during the midsummer precipitation maximum (Magaña et al., 1999; Magaña et al., 2003). Similarly decreases in winter temperatures throughout northern Central America have been shown to be affected by the prevalence of cold surges, or nortes, that originate in the northern mid-latitudes of North America. The cold surges have been linked with anticyclones that occur because of atmospheric turbulence east of the Rockies and the Mexican Sierra Madre (Schultz et al., 1997). Nortes can have a severe impact on Central America by

lowering temperatures, increasing wind speeds, along with associated higher pressures (Schultz et al., 1998). These surges, which are a common occurrence during the winter months lasting on synoptic timescales, could also coincide with strong El Niño years to remain as a dominant climate driver during the winter months (Schultz et al., 1998).

Regional Late Quaternary Climate

Reconstructing paleoclimate depends on a correlation between the timing of certain geological and climatological events. Following the estimates of Mark et al., (2005) the global last glacial maximum (LGM) can be defined as occurring at 21 ± 2 ka (18 ± 2 ^{14}C ka), while other reports suggest a range in the timing of a tropical maximum glacial advance covering 19 to 16 ka (Blard et al., 2007). Presented here are various estimates that fall roughly within the timeframe of the global LGM, although the term *local* last glacial maximum (LLGM) is defined herein as the northern Guatemalan highlands specific last glacial maximum.

Last glacial maximum temperature depression and precipitation estimates for both lowland and highland circum-Caribbean regions have been estimated from a variety of proxy records including lake core sediment analysis (Hodell et al., 1991, 2008; Metcalfe et al., 2002; Hillebrand et al., 2005; Anselmetti et al., 2006), paleo-vegetation changes (Leyden, 1995; van der Hammen and Hooghiemstra, 2002) and glacial geology (i.e., Stansell et al., 2007; Lachniet and Seltzer, 2002), which are summarized below.

A majority of the Central American paleo-temperature and paleo-precipitation records have been estimated to the Pleistocene/Holocene transition at ~ 11 ka (i.e., Anselmetti et al., 2006) and typically do not extend to the global LGM at ~ 21 ka. In

Costa Rica a late glacial temperature depression of 8 to 9°C from modern is reported in Lachniet and Seltzer, (2002) from glacial evidence of the LGM Talamanca stage moraines of Chirripó National Park. This estimate falls within the range reported in Islebe and Hooghiemstra (1997) who estimated a possible 6 to 9°C of cooling from fossil pollen studies carried out in Costa Rica. Data from various tropical locations provide a range of LGM temperature depression including the data of Orvis and Horn (2000) who estimated a temperature depression of 7.4 to 8.0°C from glacial ELAs with a chronology constrained by basal sediments cored from lakes beneath the upper, middle, and lower glacier limits of the Costa Rican highlands. The LGM temperature depression inferred from glacial moraines of Mexico is reported as between 5 and 9°C in Vázquez – Selem and Heine (2004). Further south the LGM temperature depression estimates are reported as 8°C for the high plains of Bogotá, Eastern Cordillera, Columbia (Mark and Helmens, 2005) and $8.8 \pm 2^\circ\text{C}$, estimated from a glacial geologic reconstruction of the Cordillera de Mérida in the Venezuelan Andes (Stansell et al., 2007).

Late Quaternary paleoclimate reconstructions for Guatemala have relied upon terrestrial sediment core analysis of various locations within the lowland Yucatan Peninsula. Lake Petén Itzá, Guatemala (Anselmetti et al., 2006; Hillebrand et al., 2005; Hodell et al., 2008), Lake Quexil, Guatemala (Leyden, 1995) and other studies from the northern Yucatan Peninsula (i.e., Leyden, 2002, Hodell et al., 2007)). Little to no data is available to constrain the northern Guatemalan highland temperature and precipitation values. A paleo-vegetation study by Leyden, (2002) estimated a late Pleistocene (~24 to 14 ^{14}C ka) temperature depression of 6.5 to 8°C for the Mayan lowlands from Lake Quexil, Guatemala. Deep water cores from Lake Petén Itzá indicate a warmer, wetter

climate ~11.3 ka following the glacial period (Hilleshien et al., 2005). Although these data suggest a cooler climate during the Late Quaternary in Guatemala, there remains minimal evidence for glacial age temperature and precipitation values in the northern highlands where actual glacial evidence is found. Recently, work by Hodell et al. (2008) on Lake Petén Itzá sediment cores reported that the LGM (23 to 19 ka) was a moist period in the Guatemalan lowlands and Yucatan Peninsula which was derived from increased summer precipitation related to a northerly inter-tropical convergence zone (ITCZ) and/or winter precipitation related to the nortes cold surges, switching to drier conditions at ~18 to 14.7 ka.

Recent studies of marine sediments from the Cariaco basin, north of Venezuela (Fig. 1), illustrate that the latitudinal shift of the ITCZ is linked to changing precipitation in Central America (Peterson and Haug, 2006; Peterson et al., 2000) and may affect climate in this region. It was shown that during cold stadial periods, such as the last glacial, a southward shift of the ITCZ was associated with a decrease in precipitation to northern South America and Central America. In Guatemala, greater moisture availability was likely related to increased winter precipitation associated with frequent polar outbreaks, combined with an increase in northerly winds which even today intermittently increase precipitation and reduce temperature in northern Guatemala during the boreal winter.

Studies of Barbados coral reefs, which utilized both O isotope and Sr/Ca thermometry (Guilderson et al., 1994), indicate a sea surface temperature reduction of ~5.0°C at 18 to 19 ka relative to the CLIMAP, (1976, 1981) sea surface temperature depression estimates of 1.4 to 1.7°C which were calculated via planktonic microfossil assemblages.

Guilderson et al., (2001) employed $\delta^{18}\text{O}$ analysis to calculate a tropical Atlantic sea

surface cooling of 4.5°C which is centered on ~ 19 to 24 ka. A similar study postulates that a reduction in global thermohaline circulation (THC), that ultimately affects north Atlantic climate, would have had a reverse effect essentially trapping heat in the tropics (Leduc et al., 2007). That increased heat would drive increased evaporation of the Caribbean and Gulf of Mexico, possibly affecting precipitation input to the Guatemalan highlands. Other work in Mg/Ca thermometry (Lea et al., 2000) reveals a late Pleistocene sea surface temperature reduction of $2.8 \pm 0.7^{\circ}\text{C}$ for the tropical Pacific, which includes both eastern and western Pacific locations. The affect of the tropical Pacific on forcing climate in Central America is unresolved since the changing sea temperatures may be related to the El Niño/southern oscillation or even Antarctic influences. A study of faunal assemblages by Mix et al. (1999) reported an ice age sea surface temperature estimate of -5 to -6°C from present in the equatorial Atlantic and eastern Pacific oceans while another study utilizing sea sediment and planktonic records from the Caribbean estimates a tropical cooling of 4°C (Lea et al., 2003). The variations in both terrestrial and ocean temperature estimates suggest that supplementary proxy records are necessary for completing a more detailed record of the tropical LGM climate.

Estimating the Equilibrium Line Altitude (ELA)

In the tropics the equilibrium line altitude (ELA) typically coincides with the $0 \pm 1^{\circ}\text{C}$ isotherm in the atmosphere, especially for a humid inner-tropical zone like Guatemala (Benn et al., 2005). Due to this atmospheric consistency an estimate of temperature change can be determined via an altitudinal change of the paleo-equilibrium line (ELA_p)

from the current position (ELA_c). That change can be calculated from the simple equation:

$$ELA_c - ELA_p = \Delta ELA$$

By calculating the ΔELA , or ELA depression from present to the past, an estimate of paleotemperature depression (ΔT) can be calculated from a known temperature lapse rate (T_1), such that:

$$\Delta ELA * T_1 = \Delta T$$

On a glacier surface the ELA represents the 'snow line' or boundary between areas of ablation and accumulation on the glacier (Fig. 4). Even though there is a direct relationship between changing climate and a change of the position of the ELA (i.e., Benn and Evans, 1998), the independent influences of precipitation and temperature on the glacier mass balance may be difficult to deconvolve (Benn et al., 2003; Benn and Evans, 1998; Kaser and Osmaston, 2002). Several qualitative methods have been proposed for estimating the ELA of paleo-glaciers, some of which are presented in this study. For a full account of methods that calculate the paleo-ELA see Porter (2001) and Osmaston (2005).

The most widely used methods for estimating the ELA of paleo-glaciers, provided good physical evidence or maps are available, are the terminus-headwall altitude ratio (THAR), the accumulation area ratio (AAR) and the area altitude balance ratio (AABR). Although each method has been utilized in variety of regions (Benn and Evans, 1998; Kaser and Osmaston, 2002) the AABR method, which takes into account the glacier area, elevation and the vertical mass balance gradient, is considered the most accurate method for estimating paleo-ELA (Osmaston, 2005).

The THAR method assumes that the ELA corresponds to some fixed ratio between the elevation of the glacier terminus (E_t) and the headwall (E_h) for mountain glaciers. The ELA estimated from THAR can be calculated by:

$$ELA = [(E_h - E_t) * THAR] + E_t$$

Research on glaciers located in tropical regions have yielded a range of THAR values from 0.2 to 0.5 (Kaser and Osmaston, 2002) which means that the ELA is 20 to 50% higher in elevation than the toe of the glacier, in contrast a THAR of 0.35 to 0.4 is typically used for mid-latitude glaciers (Benn and Evans, 1998). The AAR method utilizes an assumed ratio of the accumulation area to total area of the glacier surface. The AAR can be estimated from the following simplified equation:

$$AAR = S_c (S_c + S_b)^{-1}$$

Where S_c is the area of the accumulation area and S_b is the area of the ablation area on the glacier surface. A value of 0.6 to 0.7 has been shown to be the most widely used value although higher values (i.e., 0.8) have been shown to better represent glaciers in tropical regions (Kaser and Osmaston, 2002). The AAR method, unlike the THAR method, takes into account the glacier hypsometry (glacier area vs. altitude) giving a more accurate representation of the shape of the glacier which can impact ice reconstruction efforts. Although the AAR method is more accurate, studies show that debris rich glacier surfaces could lower AAR values significantly, thereby complicating ELA estimates if that information is unknown (Benn et al., 2005).

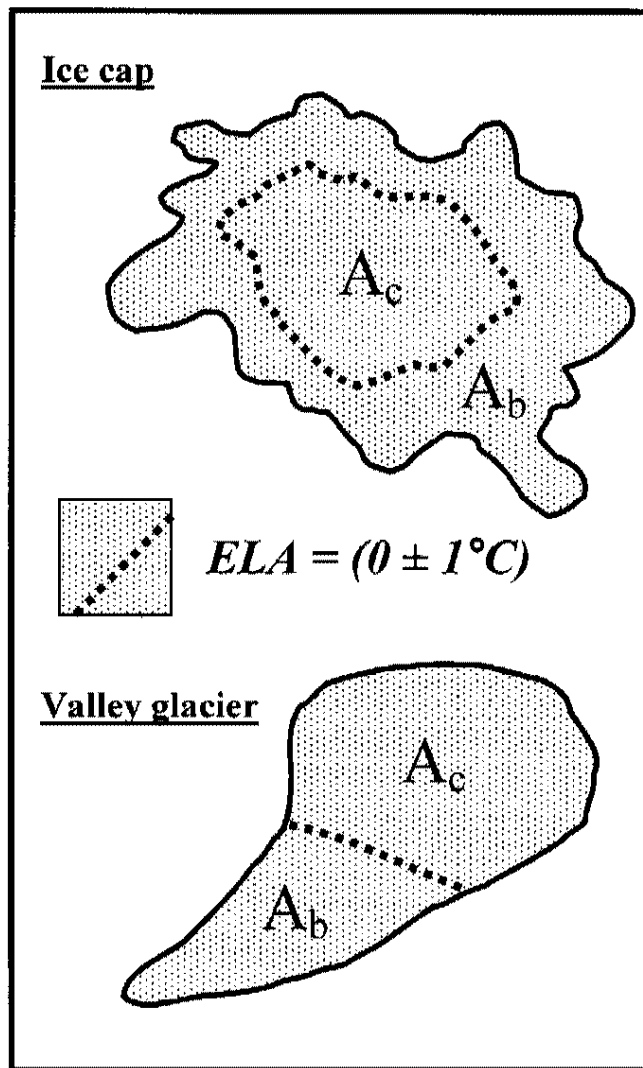


Figure 4. A map-view diagram of the accumulation A_c and ablation (A_b) areas found on an idealized ice cap and cirque or valley glacier. The boundary between the two regions is the equilibrium line altitude (ELA) which corresponds to the $\sim 0^\circ C$ isotherm in the tropical atmosphere.

The AABR method applies the vertical mass balance gradients (mm/m) of the accumulation area and ablation area to calculate a balance ratio for a specific glacier (Benn and Evens, 1998; Osmaston, 2005). On the glacier surface the accumulation and ablation gradients can vary and are controlled primarily by changes in precipitation and temperature. In the tropics the vertical mass balance profile has a strong gradient below the ELA and weak gradient above the ELA due in part to the year-round ablation common to tropical glaciers (Kaser and Osmaston, 2002; Benn et al., 2005). It becomes an important aspect of glacier reconstruction efforts to include the vertical mass balance gradients and calculate a balance ratio for specific glaciers. For a rectangular slab shaped glacier the balance ratio (BR) can be calculated from:

$$BR = b_b / b_c$$

where b_b is the mass balance gradient for the ablation area and b_c is the gradient of the accumulation area, typically measured in mm water equivalent / m elevation. The BR typically increases equatorward from the poles although most reviews of published tropical glacier studies used a BR = 2 to 4 (Benn and Evans, 1998; Benn and Gemmel, 1997; Mark et al., 2005; Kaser and Osmaston, 2002).

Central American Late Quaternary ELAs

Past published glacier reconstructions for the Sierra de los Cuchumatanes (Anderson, 1969a, b; Hastenrath, 1974; Lachniet and Vázquez-Selem, 2005) have been based primarily upon limited field evidence, combined with a broad reconstruction of ice extent using established methods mentioned above. Initial calculations of the Guatemalan ELA and estimation of maximum ice extent were carried out by Lachniet and Vázquez-Selem

(2005) to reconstruct the LLGM extent and ELA using the modified ice limits of Anderson, (1969a, b) and Hastenrath, (1974). The estimated Guatemalan ELA_{LLGM} is 3655 m and 3544 m using THAR values of 0.5 and 0.2 respectively. Based on the present day 0°C isotherm of 4900 ± 200 m in Costa Rica and Mexico, a Guatemalan highland ELA_{LLGM} depression of 1300 to 1500 m was calculated (Lachniet and Vázquez-Selem, 2005).

The glaciers of Mexico are well documented, occurring mainly across the Trans-Mexican volcanic belt (TMVB) in central Mexico. Glacial geologic studies report evidence for modern highland glaciation (e.g., Iztaccíhuatl, Popocatepétl) and up to 5 or 6 different glacial advances since the LLGM for other Mexican locations (e.g., Volcán Ajusco) (White, 1981; 1986; 2002; White and Valastro Jr., 1984, Vázquez-Selem and Heine, 2004). The mean ELA_{LLGM} in the TMVB, calculated from 20 glaciers, is 3650 ± 140 m, 3940 ± 130 m and 4090 ± 130 m for THAR values of 0.2, 0.4, 0.5 respectively (Lachniet and Vázquez-Selem, 2005). The timing of the two major late glacial advances, named Hueyatlaco -1 and Hueyatlaco -2 was ~ 20 to 17.5 ^{36}Cl ka and ~ 17 to 14 ^{36}Cl ka respectively (Vázquez-Selem and Phillips, 1998). Based on modern ELA estimates of 4900 to 5000 m the ELA_{LLGM} depression is calculated to be 1000 to 1300 m, although geomorphological evidence from Volcán Ajusco indicates as much as 1500 m of ELA lowering could have occurred from the pre-LGM and late glacial advances (Vázquez-Selem and Heine, 2004; Lachniet and Vázquez-Selem, 2005).

In the Cordillera de Talamanca, Costa Rica, glacial geologic studies report that the LLGM Talamanca moraines extend from 3450 to 3040 m, along with glacial features present at ~ 3000 m (Orvis and Horn, 2000; Lachniet and Seltzer, 2002; Lachniet and

Vázquez-Selem, 2005). Estimates of paleo-ELA, utilizing the common THAR (0.5) and AAR (0.65) methods, are 3545 to 3535 m and 3420 to 3370 m respectively. Calculated from the present day tropical ELA of ~4900 m the Quaternary ELA_{LLGM} was estimated to be ~1500 m lower than present for Costa Rica (Lachniet and Seltzer, 2002; Lachniet and Vázquez-Selem, 2005).

A range of moraine elevations have been reported for the Mérida Andes of Venezuela, divided into early glacial (~2600 m) and late glacial (2900 to 3500 m) events with sufficient chronological control (Schubert and Rinaldi, 1987). Organic matter ¹⁴C dates obtained from an outwash fan constrain ice proximal sediment deposition between 19,080 ± 820 ¹⁴C yr (basal age) and 16,500 ± 290 ¹⁴C yr (deposition ceased) while basal peat from an outwash terrace provides a minimum age of deglaciation at 12,650 ± 130 ¹⁴C yr. Estimations of the LLGM ELA for two glacial sites yielded values of 3665 ± 204 m (BR = 1.8) and 3760 ± 163 m (BR = 4.0) (Lachniet and Vázquez-Selem, 2005). Assuming a modern ELA value of ~4700 m (Schubert, 1974), ELA_{LLGM} depression ranges from ~1100 m to ~1300 m (Lachniet and Vázquez-Selem, 2005). Recent work by Stansell et al, (2007) has provided more insight into the glacial geology and paleoclimate of Venezuela by estimating LLGM ELA depressions of 850 to 1420 m lower than present. Temperature depression estimates in the Venezuelan Andes during the LGM are reported as 8.8 ± 2.0°C and possibly as much as ~11°C from present when using a combined energy and mass-balance equation (Stansell et al., 2007).

CHAPTER 2

METHODS

It is essential for any study using glacial geomorphology as a proxy for paleoclimate reconstruction to utilize a variety of methods since each typically has inherent associated errors and assumptions (Benn et al., 2005). The strength of this study was the ability to utilize proven methods such as the AAR and AABR, combined with a physically based mass balance glacier model, to estimate the northern Guatemalan highlands LLGM ELA. Using a variety of ice reconstruction methods, with the use of GIS to build accurate glacial geologic maps, has been marked as a necessary step in calculating more accurate LLGM climate estimates (Mark et al., 2005; Napieralski et al., 2007).

Glacial Geology

The glacial geomorphologic and geologic field mapping of the plateau region was conducted over a 6 day period in March 2006. Extensive moraine sequences and various glacial landforms were observed and mapped along the eastern edge the San Miguel, Tuizoche and Ninguitz Valleys (Fig. 5, 6 and 7). Mapping of these sinuous moraine crests was done using a global position system (GPS) receiver (error average $\pm 4\text{m}$) which allowed geo-referenced glacial landforms to be utilized for the completion of the GIS. Moraines that appeared to represent the furthest extent of the ice cap during the

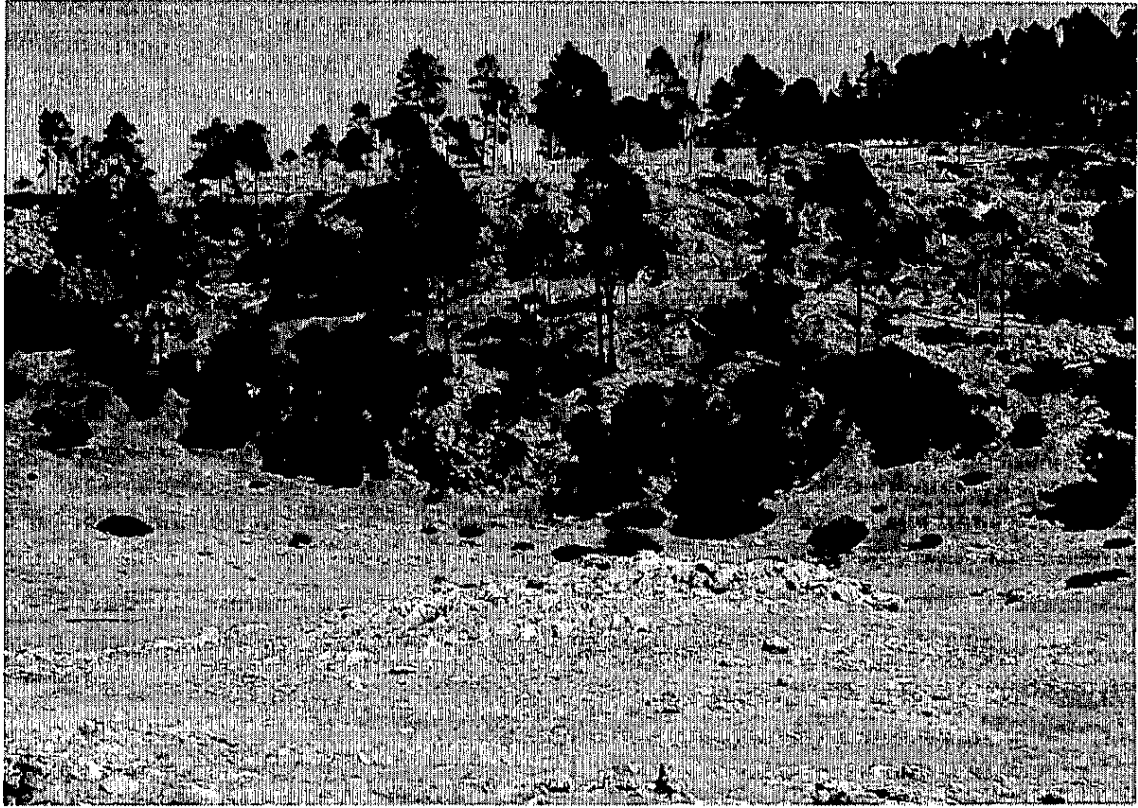


Figure 5. A small whaleback (center picture) formed below advancing ice in the eastern Ninguitz Valley, notice also the scoured bedrock surfaces and plucked lee faces of the background forested ridgeline which is a good indicator of ice flow direction and ice dynamics; photograph, Alex J. Roy

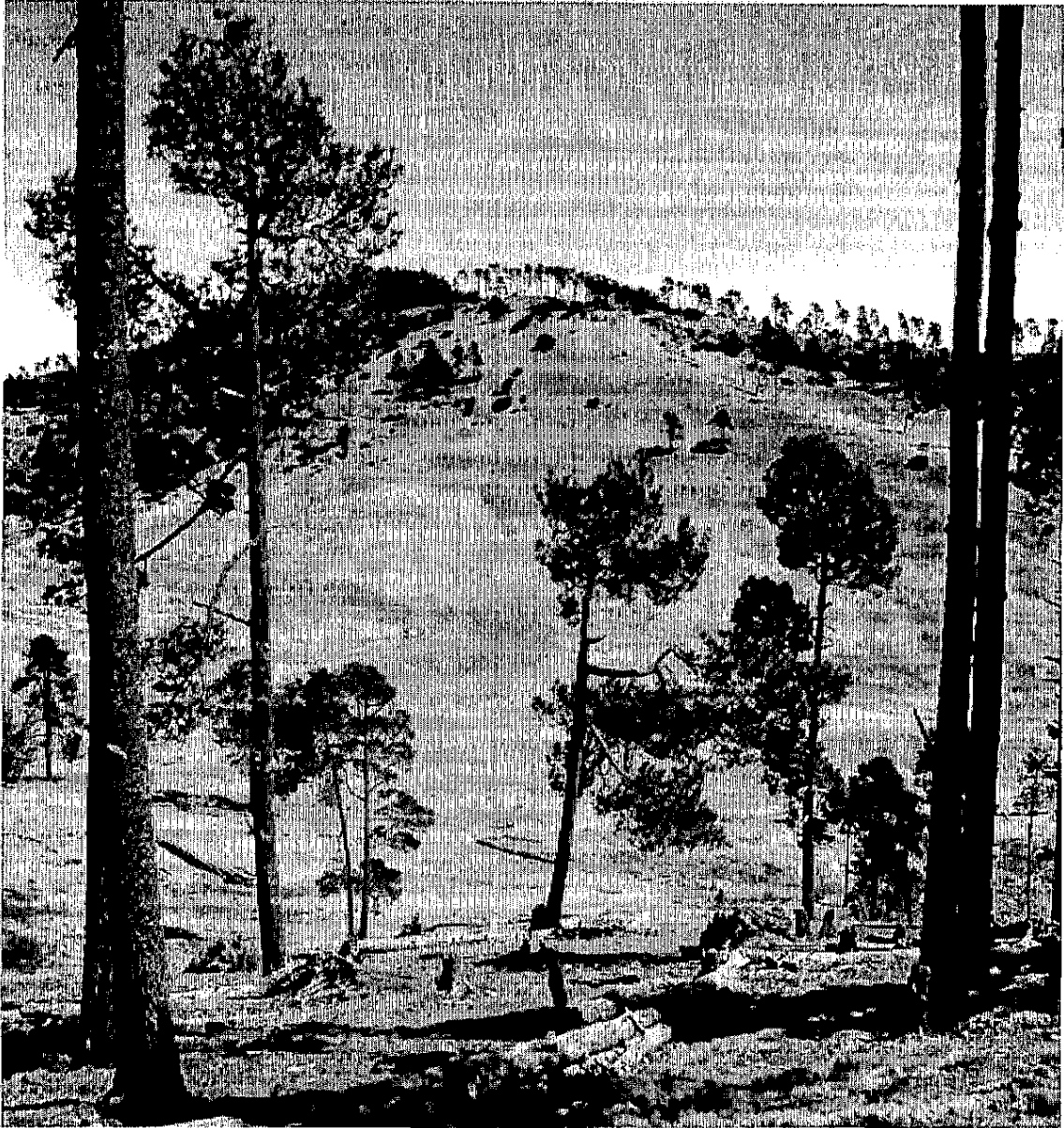


Figure 6. A large lateral moraine is evident looking north across the previously glaciated terrain of the Ninguitz Valley. Areas of scoured bedrock are visible along the bottom of the valley including smaller more muted recessional moraine segments along the valley floor; photograph, Alex J. Roy

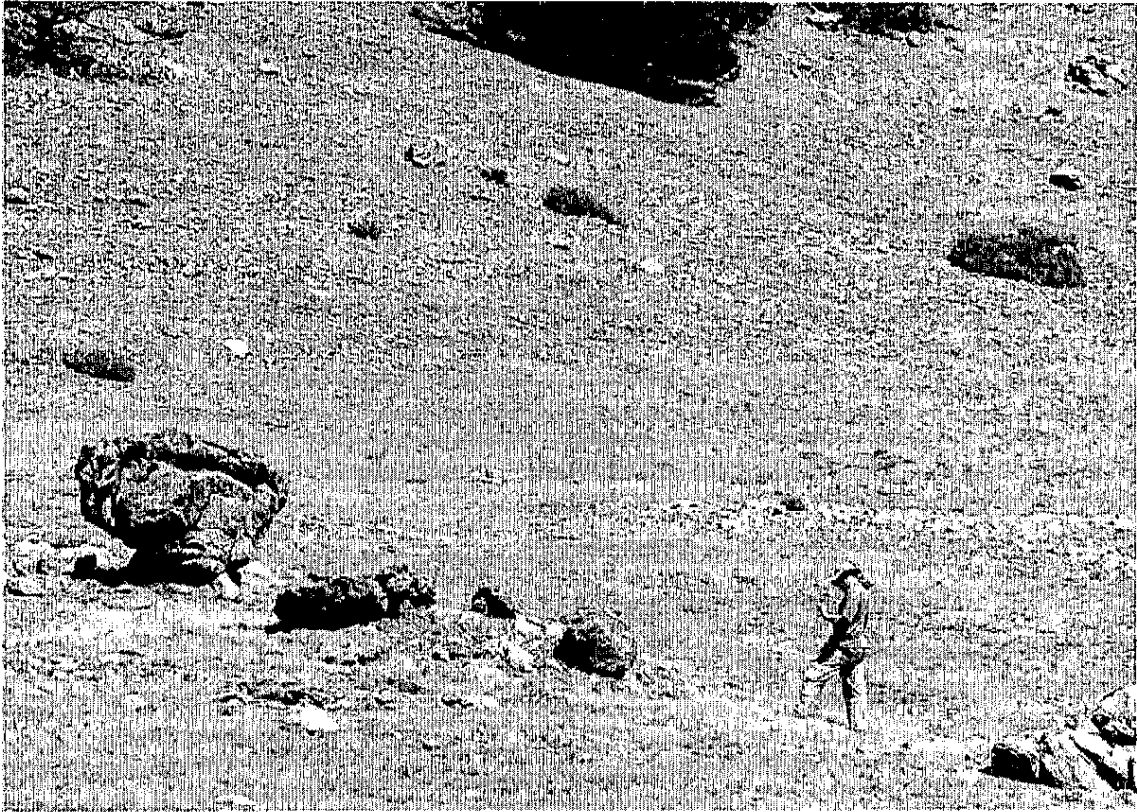


Figure 7. The author examining a deposit of large boulder sized till material at the base of eastern Ninguitz Valley. The large boulder on the left is resting on a pedestal made of till material which was deposited as ice receded; photograph, Matthew Lachniet

LLGM were mapped for ice extent reconstruction. Rock samples, for cosmogenic exposure age determination, were collected from boulders resting upon the most prominent large scale moraine crests along the eastern plateau region and accounted for a majority of the field effort. Field reconnaissance occurred primarily on the plateau region of the previously glaciated terrain, although a second trip in October, 2007 did allow further direct observation of the moraine-rich areas of the Colinas Planas. Extensive photographic evidence was taken for further morphological comparisons between the

various moraine segments and for a qualitative assessment of the ice cap and glacier dynamics.

Building the GIS

Aerial photographs, purchased from the Guatemalan National Institute of Seismology, Volcanology, Meteorology and Hydrology were used for glacial-geologic mapping in all the previously glaciated areas. The scope of the aerial photographic coverage for this field area encompassed the entire high plateau and nearby Montaña San Juan so that stereo pairs of areas that reach above the previously reported EL_{ALLGM} of ~3650m (Lachniet and Vazquez-Selem, 2005) could be examined in full detail (Fig. 8). This type of inspection enabled a comprehensive glacial geologic map of the entire field area to be created, including the ability to plot muted moraine segments and subglacial till deposits, landforms not apparent on typical topographic maps. In order to map the extensive landforms stereo-pairs were fitted with laminate covering so that the glacial features could be easily marked, along with regional geography for further spatial references. Any glacial moraines mapped in the field via GPS surveying and field location methods were utilized as a spatial reference for compiling the aerial photographic segments into a complete map. Once the entire field area was mapped with the aerial photographs the sections were scanned and digitized to be georeferenced into the GIS for completing the final map (Fig. 9).

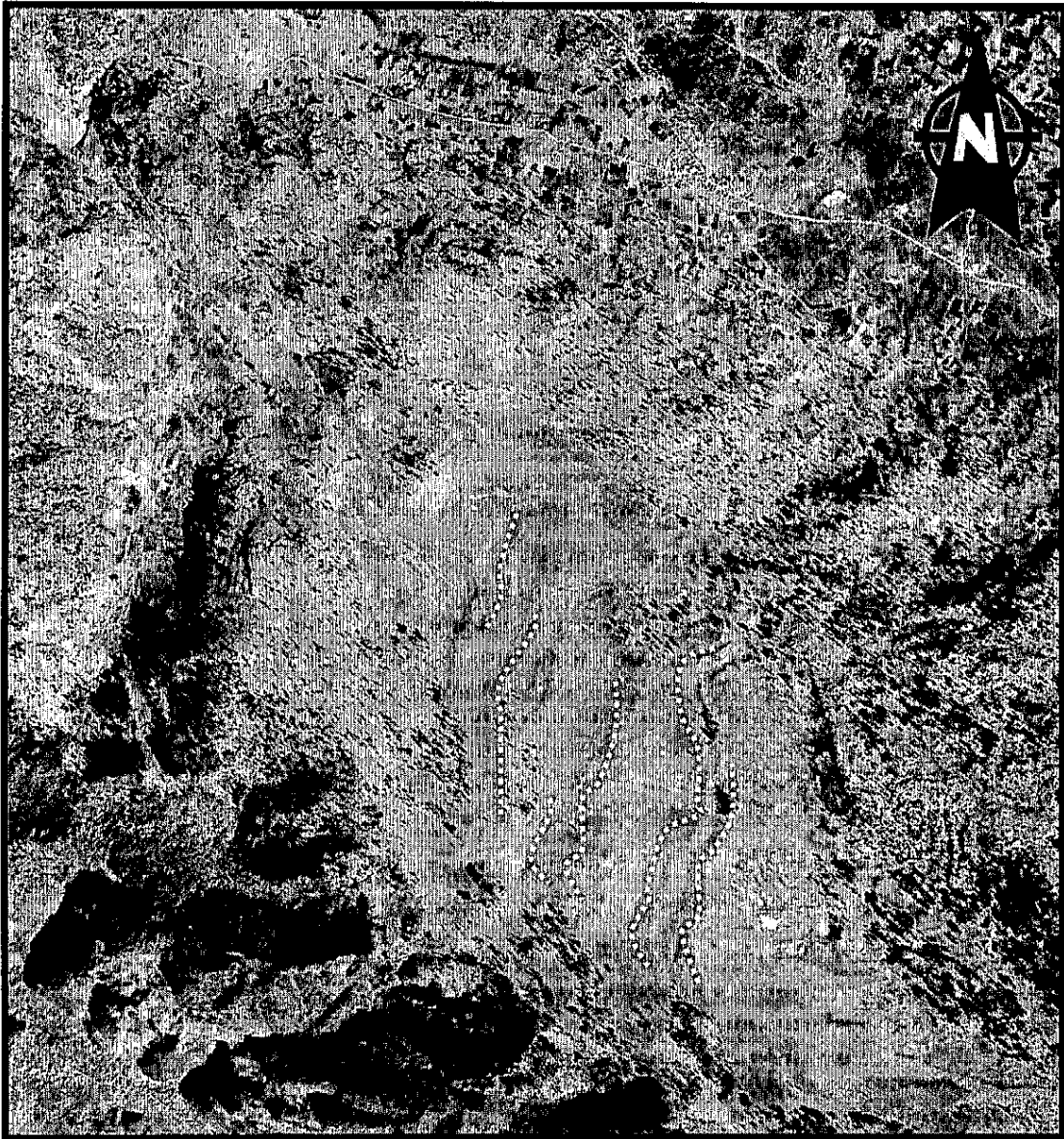


Figure 8. Shown is an aerial photograph of the western Colinas Planas region of the plateau which was used to map the extensive glacial geology of the plateau region with white dotted lines that demarcate subdued recessional moraine segments. The steep southern edge of the plateau is clearly shown along with a secondary road that runs through the field area.

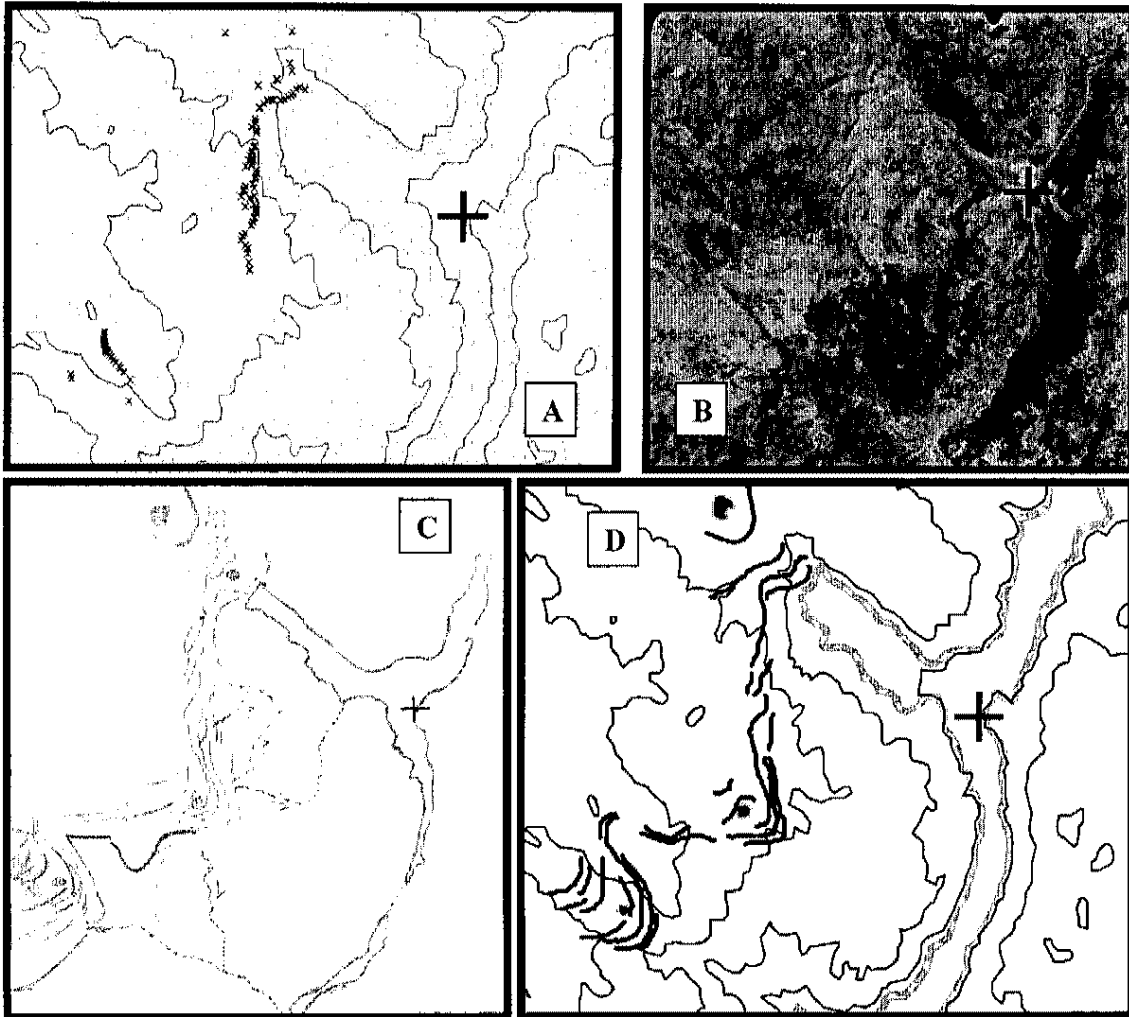


Figure 9. A graphic representation of the methods that were employed to create the final glacial geologic map; glacial evidence was field located using GPS (A); aerial photographs (B) were utilized to trace all other recognizable glacial evidence, including moraine segments and glacial outwash as shown in (C) which was then georeferenced into the GIS to create the final map (D). Black cross represents one of the georeferenced points for the plateau region.

Glacier Modeling

The glacier model employed in this study utilizes a 2-D precipitation accumulation/ablation model combined with a glacier flow model first described in Plummer and Phillips (2003). The annual net accumulation and ablation for each grid section are calculated from the energy balance of the snow surface during the melt season. The mass balance output data is then used as input for the glacier flow model. The mass balance model can determine the amount of snow that will form based on regional temperature and precipitation data, along with local aspect, shading and insolation at the field site. The digital elevation model (DEM), which is required as the baseline input for the glacier model, was compiled by hand digitizing geo-referenced 1:50,000 scale topographic maps. The resultant DEM that was produced had a 50 m resolution which provided a detailed topographic model for the cirque glacier and ice cap reconstruction. The preliminary input for the glacier model requires a DEM for hillshade analysis which measures the amount of ground surface exposure to the sun and the viewfactor which takes into account the aspect of different slopes. The GIS analysis provides a way to estimate the amount of insolation at the land surface, which affects glacier ablation and any topographic shading or aspect variations that may affect glacier dynamics.

Given that glacier dynamics are most dependant on changes in mass balance at the glacier surface, the monthly precipitation and temperature climate data were important primary inputs to the mass balance model (table 1) (Benn and Evens, 1998; Plummer and Phillips, 2003). Daily temperature and precipitation data from two Guatemalan weather stations were used as the primary input files for the GIS mass balance and glacier model.

Additional climate parameter input included mean monthly averages of relative humidity, cloudiness, and wind speed, along with the standard deviation of daily temperatures for each month. In order to calculate the local environmental lapse rates necessary for the model runs climate data was analyzed from weather stations in Todos Santos Cuchumatán and Puerto San José, the latter located along the southern Guatemalan Pacific coast. Average monthly temperature, precipitation, relative humidity, wind speed and cloudiness data were analyzed from Todos Santos Cuchumatán for the years 1990 to 2006, while only temperature and precipitation data were collected from San José for environmental lapse rate calculations.

Table 1. Climate input for the Plummer and Phillips, (2003) mass balance GIS model.

Model parameters dictate that the arrangement of the monthly climate variables starts at the beginning of the rainy season; for the northern Guatemalan highlands that is early May. Data was obtained from published web based climate records for a weather station in Todos Santos Cuchumatán (2480 m) and San José (~0 m) averaged for the years 1991 – 2003 (appendix I). T is in °C, while the Temperature Lapse Rate (TLR) is °C/m elev.

Month	Mean T	Sky Cover	Humidity	wind m/s	TLR
may	15.3	71%	85%	0.9	-0.00527
jun	15.0	74%	86%	0.9	-0.00525
jul	14.5	71%	86%	1.0	-0.00526
aug	14.4	70%	85%	1.0	-0.00513
sep	14.4	73%	88%	0.9	-0.00543
oct	13.8	71%	87%	1.2	-0.00530
nov	13.2	63%	85%	1.1	-0.00524
dec	12.8	59%	83%	1.3	-0.00546
jan	12.7	46%	83%	0.5	-0.00520
feb	13.7	38%	80%	0.8	-0.00537
mar	14.7	36%	80%	0.8	-0.00554
apr	16.0	50%	81%	1.0	-0.00544

A second temperature lapse rate and present day ELA was compiled from a data set of 64 different weather stations located throughout Guatemala (Appendix II). The data from INSIVUMEH, (2006) provides only one value per station for the average annual precipitation totals and annual daily temperature which yields a slightly steeper estimate of the temperature lapse rate at $-5.6^{\circ}\text{C}/\text{km}^{-1}$ and a present day 0°C isotherm of 4650 m (Fig. 10); this value is at the low end of the Central American present day ELA range of 4900 ± 200 m, and may represent an extrapolation error, as no climate stations were reported above ~ 2500 m altitude. Since the model input requires very specific average monthly data along with the standard deviation of the daily temperature fluctuations this second 'country average' temperature lapse rate was not input into the GIS model.

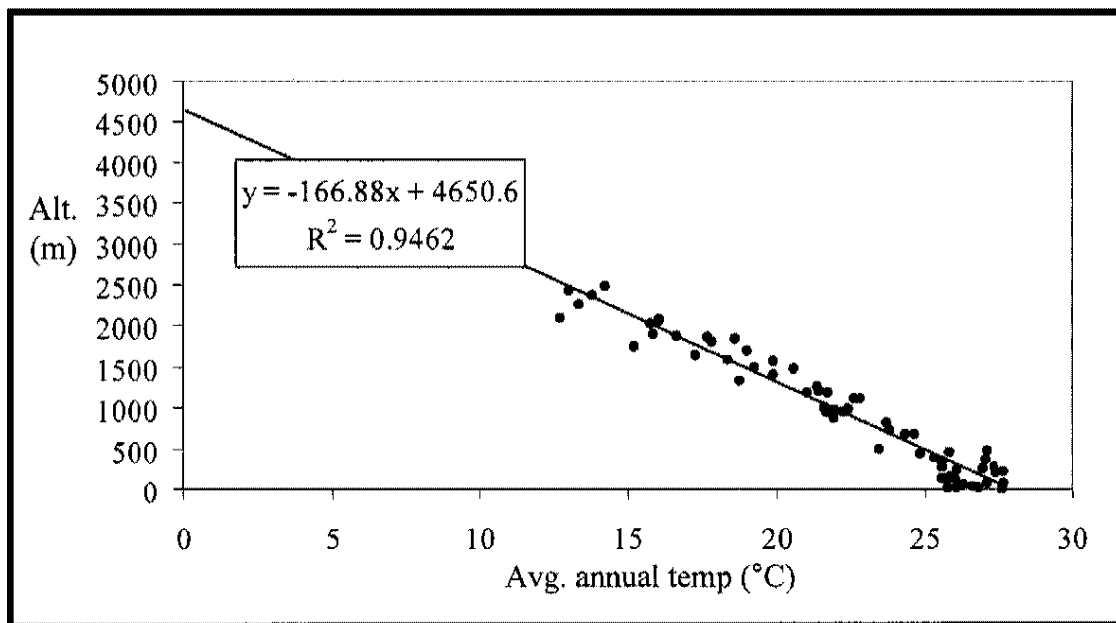


Figure 10. Plot of the average annual temperature ($^{\circ}\text{C}$) data vs. station elevation (m) from Appendix II which gives a country average present day ELA for Guatemala of 4651 m.

The GIS model takes a typical glacier reconstruction a step further by integrating the effects of topography, aspect, and changing climate with altitude, which are typically not included in the glacier reconstruction (Mark et al, 2005). To constrain the range of paleo-temperature and paleo-precipitation estimates for the northern Guatemalan highlands during the LLGM, more than 50 iterations of the mass balance model were run, some of which are given in Appendix III. Since the output of the mass balance model is gridded (raster) data, it can then be overlaid on the DEM for determination of the equilibrium line altitudes for the various model runs. The model strength also comes from the ability to compare model output to the physical data, such as moraine traces, that were mapped in the field. The mapped moraine limits were used to evaluate the plausibility of the mass balance estimates since the model output would allow a quick rejection of any estimates of positive mass balance in any mapped ice free regions. The primary output of the mass balance model is the net annual accumulation or ablation for a given grid section of the DEM. The model output permitted the areas of zero mass balance (± 100 mm water equivalent) to be contoured, thus providing an estimate of the steady state LLGM ELA (Benn and Evens, 1998; Benn and Lehmkuhl, 2000) for the particular model run. Here an increase or decrease in values of temperature, precipitation, wind speed and cloudiness, such as would occur during the LLGM, can be estimated to constrain how changes in various climate parameters affect mass balance. This gridded data of specific mass balance estimates was then utilized in building a range of temperature and precipitation estimates for the Guatemalan LLGM.

THAR, AAR, AABR and Ice Thickness

Paleoglacier ELAs for the northern Guatemalan highlands ice cap and cirque glaciers were determined using the accumulation area balance ratio (AABR), accumulation area ratio (AAR) and the terminus-headwall altitude ratio (THAR) methods (Porter, 2001; Benn and Evans, 1998; Benn et al., 2005; Benn and Lehmkuhl, 2000, Kaser and Osmaston, 2002). The AAR utilized in this study followed the estimates of Kaser and Osmaston, (2002) and Benn et al., (2005) for tropical regions to calculate the ELA of the reconstructed Guatemalan ice cap and cirques. This study used a value of 0.65 for the AAR which correlates well to other previously published estimates of the tropical 'optimum' AAR range of 0.5 to 0.7 (Kaser and Osmaston, 2002; Lachniet and Vázquez-Selem, 2005; Mark et al., 2005) .

Other ELA estimates, using the AABR method, were calculated via a balance ratio spreadsheet which allowed for the area vs. altitude of the Guatemalan glaciers to be compared to outer tropical (BR = 1.0 to 2.0) and inner tropical (BR = 2.0 to 5.0) balance ratios (Osmaston, 2005; Lachniet and Vázquez-Selem, 2005; Benn et al., 2005; Mark et al., 2005). The tropical balance ratio, like the tropical AAR, is affected by the year-round ablation and an almost constant elevation of the 0°C isotherm giving balance ratio estimates as higher in the tropics (>2.0 Kaser and Osmaston, 2002) than the mid-latitude estimate of 1.8 (Furbish and Andrews, 1984). The balance ratio assumes that for steady state conditions the total annual accumulation above the ELA must equal the total annual ablation below the ELA and can be determined from the equation (Benn and Evans, 1998):

$$d_b A_b = d_a A_c$$

Where d_b and d_c are the average net annual ablation and accumulation respectively, and A_b and A_c represent the area of the ablation and the accumulation area respectively. Another assumption is that typically the vertical mass balance gradients above and below the ELA is linear, so both d_b and d_a are equal to z_b and z_a which represent the ablation/accumulation at the area weighted mean elevation of the ablation/accumulation area. For steady state conditions the ELA can then be determined by the balance ratio according to the relationship:

$$b_{ab} / b_{ac} = z_c A_c / z_b A_b$$

By convention z_b and z_c are associated with the $\frac{1}{2}A_b$ and $\frac{1}{2}A_c$ elevations, such that the ELA can be determined from either assuming a typical BR (i.e., from mid-latitudes, tropics) or to measure the mass balance ratios from direct field observations or glacier modeling (Benn and Evans, 1998). Due to the year-round ablation and homogeneous atmosphere of the tropics, balance ratios of 1.0 to 25 were used to determine the LLGM ELAs, although for this research values that range from a BR = 2.0 to a BR = 4.0 were determined to fit this tropical highland region based on previous studies in the circum-Caribbean region (Lachniet and Vázquez-Selem, 2005).

Although the toe-to-headwall altitude ratio (THAR) provides a crude estimation of the ELA, it did allow for an immediate estimate of the entire Plateau region and Montaña San Juan. A THAR value of 0.4 is typical for tropical regions although further research suggests that this value can change depending on the shape of the glacier or the size of the discharge area; higher values were used (0.46 to 0.57) to estimate the ELA of the tropical Rwenzori glaciers in Africa (Kaser and Osmaston, 2002) while lower values (0.35 to 0.4) may be used for mid-latitudes (Benn and Evans, 1998). Following estimates

of the tropical THAR a value of 0.4 was determined to be a good average (Kaser and Osmaston, 2002), which also correlates to local glacial studies of Mexico and Costa Rica (Lachniet and Vázquez-Selem, 2005; Mark et al., 2005).

The maximum extent of the ice cap and cirque glaciers were contoured via field evidence and glacial geologic mapping. Basal shear stress calculations were used to determine the plausibility of the ice reconstruction. Following the methods of Paterson (1981) and Benn and Evans (1998), glacier ice thickness can be calculated by the relationship between the slope of the glacier and bedrock surface and the density of ice. Based off the simplified glacier basal shear stress formula from Benn and Evans, (1998),

$$\tau = \rho_i gh \sin a$$

where τ is the shear stress, ρ_i the density of ice ($\sim 900 \text{ kg m}^{-3}$), g the gravitational acceleration (9.81 m s^{-2}), h is the ice thickness (m) and a is the surface slope of the ice given in degrees. For a glacier sliding on its bed the average range of potential basal shear stress values is from 50 to 150 kPa (Paterson, 1981), while a slightly lower range is found in Seltzer (1992) who estimated only 40 to 120 kPa. The basal shear stress ranges provide constraints on the amount of ice, or ice thickness, for a given slope. A spreadsheet was created for the basal shear stress calculations since the slope of glaciated surfaces ranged from 1 to 55° based on topographic cross sections of the plateau region and the Montaña San Juan. Another application of this method can be found in Stansell et al., (2007) which utilized the comparable methods of Seltzer, (1992) to calculate the basal shear stress and ice thickness for the glaciers of the Cordillera de Mérida, Venezuela.

CHAPTER 3

RESULTS

Glacial geologic mapping, utilizing GPS location and aerial photographic analysis, was conducted in the eastern portions of the San Miguel, Tuizoche, and Ninguitz Valleys along with exploration of the Ventura Valley and the northern Buena Vista Ridge. Glacial landforms that were mapped solely by stereo-photographs were compared to field-located glacial landforms to assure correct interpretation of glacial deposits from the stereo-photographic analysis. Aerial photographs also present a spatial reference between the GPS located moraine crests mapped in the field and the moraines plotted via aerial photographic analysis. Since there are inherent errors (i.e. scale changes) from the distortion of aerial photographs (Bolstad, 2005), geo-referencing glacial evidence was an iterative process which combined GPS located moraine crests, aerial photographic overlays and photographic evidence to construct the final glacial geologic map and to estimate the maximum ice extent.

Glacial Geomorphology

Two prominent moraine groups were observed based on relative size and moraine crest morphology. The first moraine group consists of large terminal and lateral moraine

segments which dominate the eastern valleys of the plateau region (Fig. 11). The second types of moraine segments are smaller, muted recessional moraines which are typically

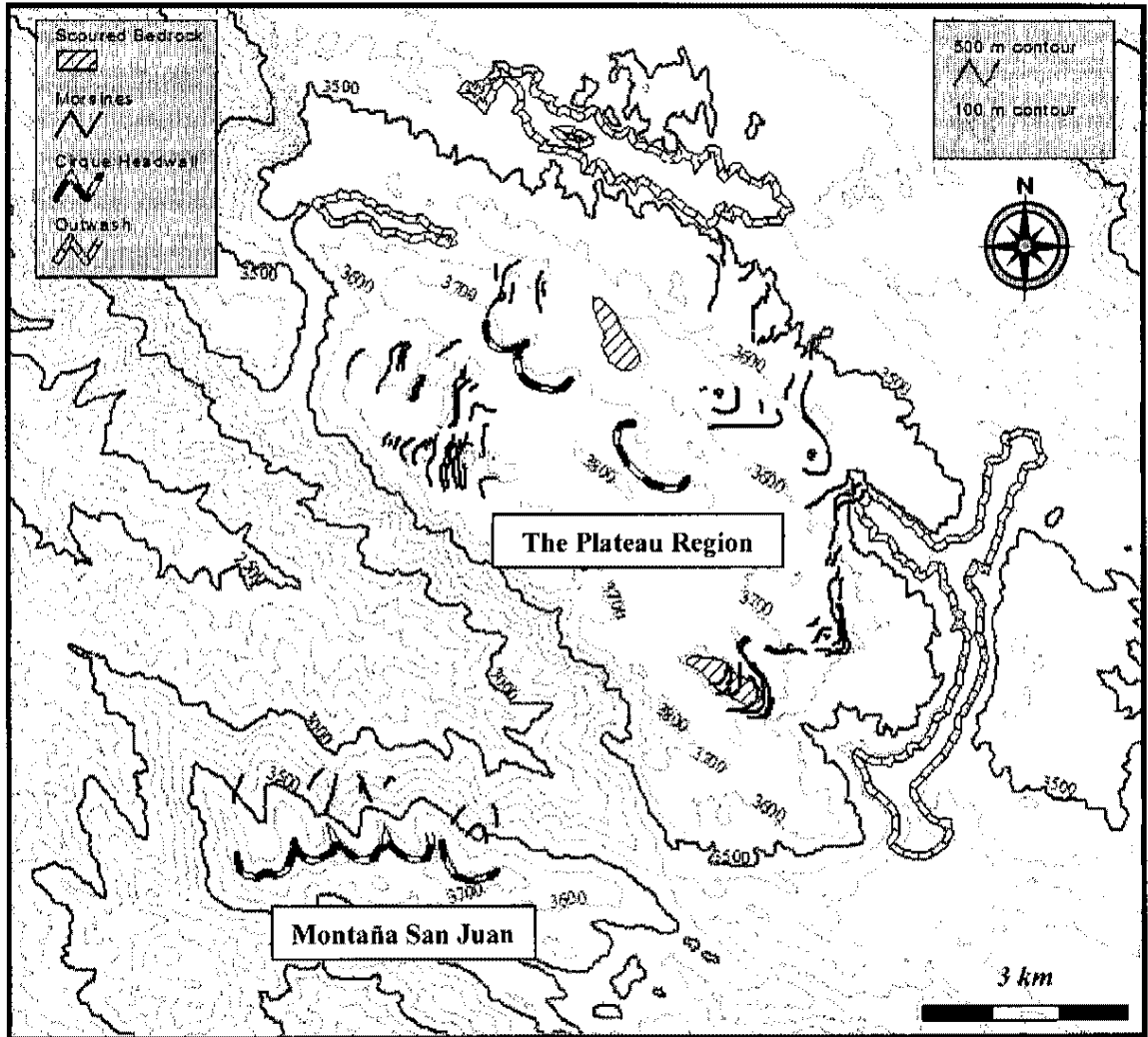


Figure 11. Topographic map of the plateau region and Montaña San Juan along with the location of mapped moraines, glacial outwash and cirque headwalls. Scoured bedrock surfaces mapped here represent large tracts of glacial scour; smaller areas, not marked, are present throughout the region.

found up-valley from the larger eastern plateau moraine segments and nested in groups across a large portion of the Colinas Planas. The larger moraine segments typically have distinctly peaked crests while some, interpreted as a possibly older sequence, are observed with more rounded broad crests. Most of the larger moraine segments were boulder rich (size >1m) although most were cobble and gravel covered. The larger moraine segments range in height from >5 to 15 m and some of the eastern valley moraines, most notably in the Tuizoche Valley, are double crested, suggesting successive steady state glacial events that advanced to the same terminus position. Further work may help in delineating additional or sequential moraine groups.

A soil horizon above San Miguel Valley till deposits was viewed from a road cut through a prominent end moraine segment and averaged ~3 to 4 cm with some areas as thick as ~10 cm above the till. The largest moraine segments found along the eastern valleys of the plateau region indicate past steady state positions of the large ice cap. Along the eastern portion of the San Miguel Valley the large moraine segments include a valley-wide end and left-lateral moraine sequence that display well defined crests, with gentle relief and slopes; the boulder-rich moraines were utilized for sampling of material for potential cosmogenic exposure age determination. A majority of large the eastern valleys moraine segments had a minor cover of evergreen trees and grass, with small cobble and gravel deposits. Evergreen trees were said to have been more prevalent than recent but were removed over time for local animal husbandry (Ramírez, pers. comm., 2006). Smaller more muted moraine segments up valley of the prominent end moraines in the eastern Ninguiz Valley and the western Colinas Planas are likely recessional. Across the plateau there are extensive scoured bedrock surfaces, although they typically lie at the

base of the valleys which have very little soil development and only grass type vegetation.

The varied scoured surfaces and erosional glacial landforms allude to the dynamics of glaciation in this region and allow for ice flow direction to be determined. Most valleys show the characteristic U-shape form along with the common lee side plucked bedrock surfaces and erosional and depositional bed-forms; all of which provide further constraints on ice flow direction of the plateau ice cap. Post-glacial landscape modification of the easily eroded limestone bedrock has resulted in the chemical erosion of striations. Only a few striated boulders were observed from recently quarried till material, while most exposed boulders and non-scoured bedrock outcrops were covered in carbonate dissolution forms such as rillenkarren furrows. Rillenkarren furrows formed in boulders perched along moraine crests provide evidence of the relative stability of these deposits if the furrows cut into the boulders were roughly perpendicular to the ground surface.

Ice Cap and Cirque Glaciers

The plateau region of the Sierra de los Cuchumatanes supported an ice cap $\sim 40 \text{ km}^2$ along with smaller cirque glaciers and nivation basins or perennial snow fields along the northern facing slopes of the Montaña San Juan (Fig. 12). The eastern half of the plateau supports the most prominent and large-scale glacial moraine segments easily observed as a continuous band extending from the northern San Miguel Valley to the southern Ninguitz Valley. The central portion of the plateau, which consists of two relatively

parallel broad U-shaped valleys, is dissected by a ridgeline of high prominent peaks and the highest point of the plateau region (3837 m). Based on aerial photographic

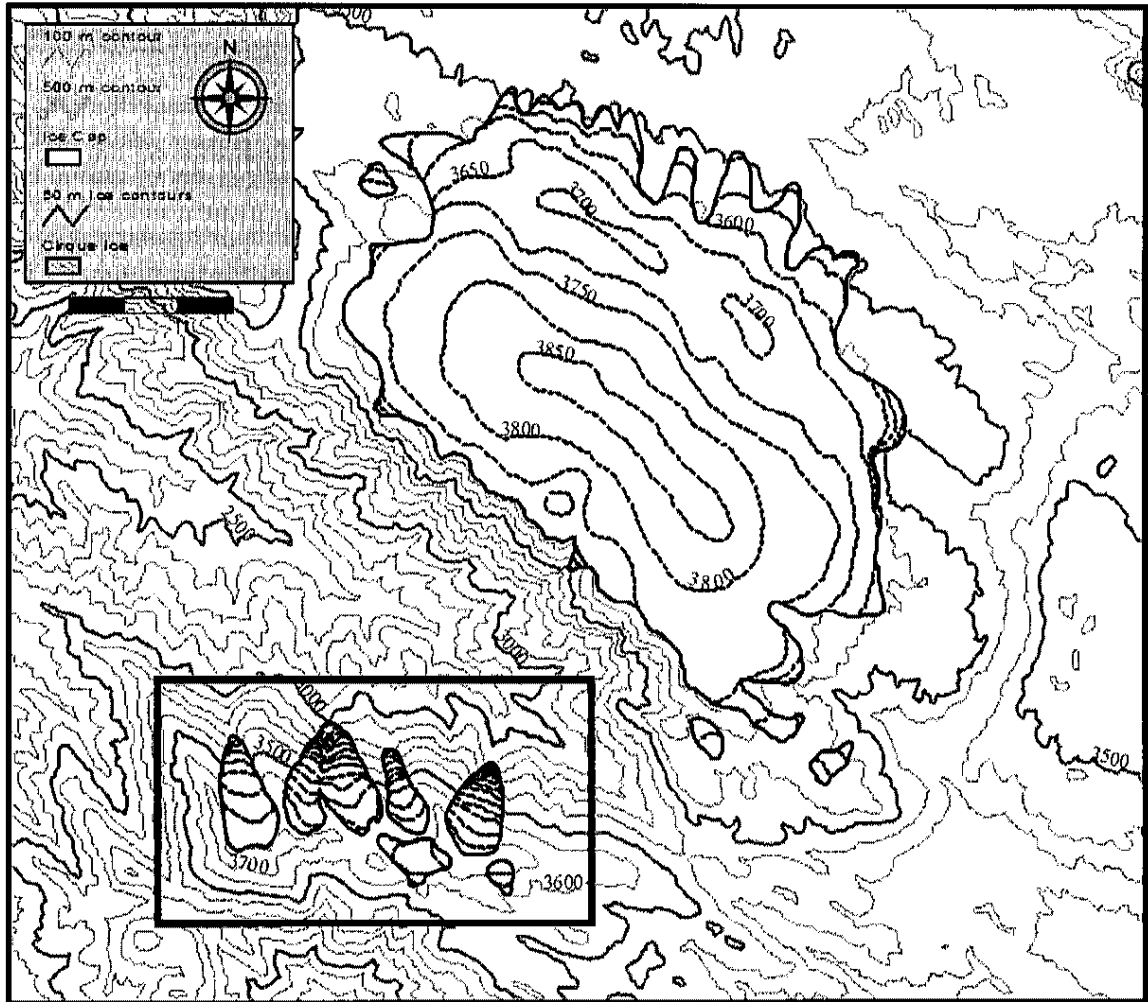


Figure 12. Map of the reconstructed Mayan ice cap and cirque glaciers (black box shown in Fig 13). Ice limits are based on mapped maximum moraine limits and glacial geomorphology. The ice contours (black dashed lines) have a contour interval of 50 m for an enhanced representation of ice thickness. Scale bar below key is equal to 3 km.

analysis the central portion of this high limestone plateau shows evidence of three possible late-stage cirques that supported ice that flowed into the confluence between the Ventura and San Miguel Valleys. The topographic and aerial photographic observations suggest that these late-stage cirques deposited moraine evidence over the large ice cap subglacial till deposits. Field evidence from the broad San Miguel and Ventura Valleys included exposed areas of glacially scoured limestone bedrock along with widespread subglacial till deposits. The eastern region of the plateau consists of a large outwash plain which constrains paleodrainage of the San Miguel, Tuizoche and Ninguitz Valley tongues of the ice cap. Additional outwash deposits were also observed in the E-W trending Chemal Valley north of the Buena Vista Ridge (Fig. 3), as based on aerial photographs. Deposits of unconsolidated material, considered subglacial till, were observed at the western edge of the Ventura Valley. A thorough reconnaissance revealed no clear recognizable moraines in the western region of the Ventura Valley. Buena Vista Ridge, a heavily scoured low relief region on the plateau, was observed with glacially plucked surfaces, including *roche moutonnées* that descend into Chemal Valley to the north. Although agriculture dominates the landscape obscuring small scale landforms, minor segments of lateral and end moraines were mapped which constrain the maximum ice extent.

The Montaña San Juan, which was mapped entirely from aerial photographic analysis, is comprised of an east-west trending rounded mountain ridge ~3700 m a.s.l flanked by a group of compound cirques which scallop the north facing slopes (Fig. 13). From the aerial photographs the small valleys below the main cirques contain small lateral and end moraine segments, although further evidence of glacial forms may be

concealed within shadowed regions of the aerial photographs. The limit on the glacial geologic mapping of the Montaña San Juan was mainly due to the lack of direct field observations and glacial evidence or landforms too small to be recognized in the aerial photographs. A high overlook on the southern edge of the plateau region named “La Torre” enabled a limited view of the cirques of the Montaña San Juan across the valley.

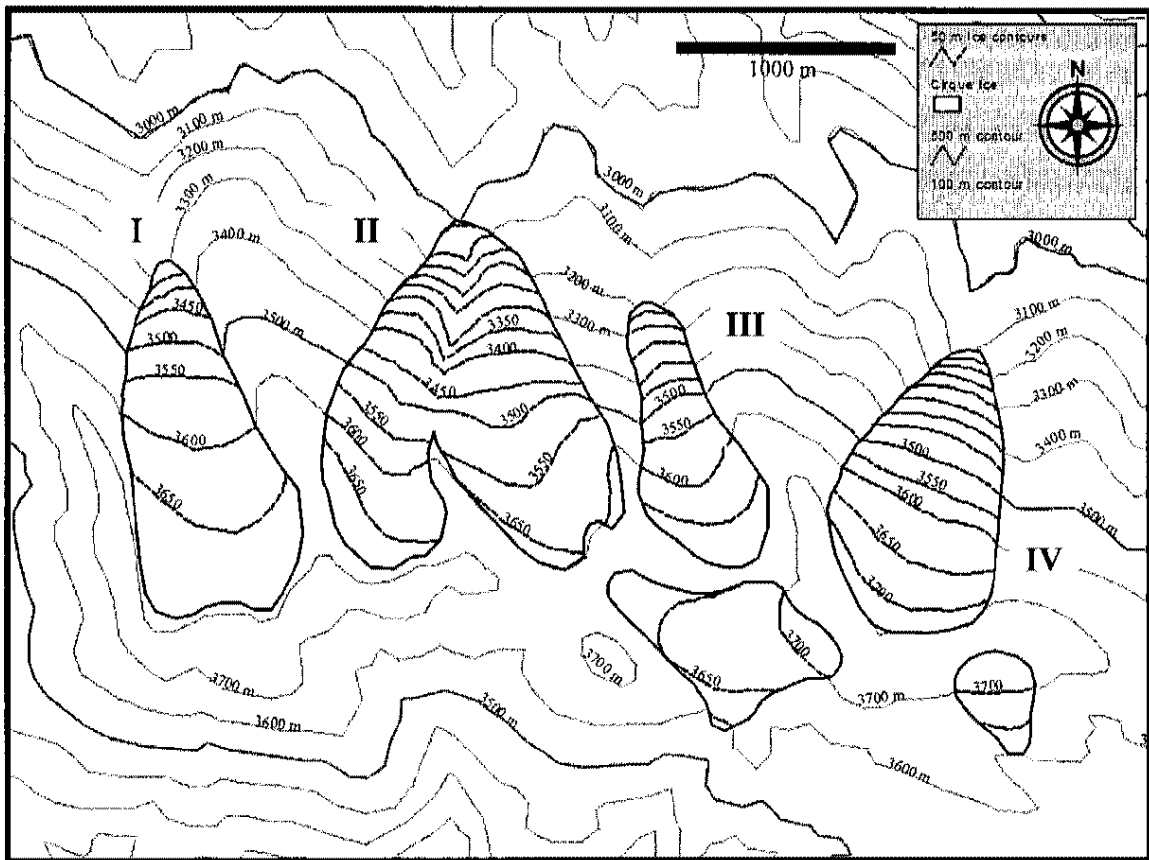


Figure 13. Map of the reconstructed cirque glaciers and snow fields outlined in Figure 12 located south of the main plateau field area on the Montaña San Juan. Ice contour intervals are 50 m, the cirque glaciers are marked with roman numerals (I to IV) as described in the text.

Photographic evidence shows these cirques as shallow basins with limited large scale landforms. Investigation of the aerial photographs also reveals that areas above the estimated equilibrium line altitude which showed glacial weathering or glacial sediments may have supported persistent snowfields or smaller nivation basins around the periphery of the ice cap and along the southern edge of the Montaña San Juan.

Past and Present ELAs

Equilibrium line altitude (ELA) estimates were made following the methods described previously (i.e., Kaser and Osmaston, 2002; Lachniet and Seltzer, 2002; Stansell et al., 2007; Benn and Evans, 1998). The values for each ratio depends on the size, shape and mass balance gradients of each glaciated region as a result employing multiple techniques provides the best constraint of the ice cap and cirque paleo-ELAs.

There is good internal consistency between the estimate of the Guatemalan LLGM ELAs when using the AABR and AAR methods. The LLGM $ELA_{BR=2}$ estimate of 3703 m for the plateau ice cap and 3515 m for the cirque glaciers is similar to the LLGM $ELA_{AAR=0.65}$ of 3650 m for the ice cap, while the cirque average is again >150 m lower at 3491 m. Because of the small altitudinal range between the lowest and highest elevation of glacial evidence of the plateau (3470 to 3840 m) and cirque glaciers (3200 to 3700 m) these LLGM ELA estimates are well constrained. The ELAs of the plateau ice cap and cirque glaciers were markedly different, in some instances the ice cap ELAs were as much as 200 above the cirque glaciers. The affects of a north facing aspect on the Montaña San Juan is apparent by the presence of these cirques and the difference between the LLGM plateau and cirque ELAs.

Table 2. Equilibrium line altitude (ELA) estimates (m) for the plateau ice cap, each cirque glacier (I to IV) and the cirque mean. These data show LLGM ELAs of ~3500-3700 m

Glacier	THAR = 0.7	THAR = 0.5	AAR = 0.6	AAR = 0.65	BR = 1.0	BR = 2.0
I	3563	3480	3550	3535	3600	3576
II	3479	3345	3460	3440	3491	3445
III	3516	3420	3510	3500	3552	3515
IV	3522	3400	3510	3490	3562	3523
Ice Cap	3715	3625	3660	3650	3727	3703
Cirque Mean	3520	3411	3508	3491	3551	3515

Table 3. Estimates of the Δ ELA (± 200 m) for the plateau ice cap, cirque glaciers and cirque mean using the present day Central American ELA of 4900 m. The cirque glaciers consistently show Δ ELA that is ~150 to 200 m lower than the ice cap estimates; due in part to the effects of aspect on perennial ice.

Glacier	THAR = 0.7	THAR = 0.5	AAR = 0.6	AAR = 0.65	BR = 1.0	BR = 2.0
I	1337	1421	1350	1365	1300	1324
II	1421	1555	1440	1460	1409	1455
III	1384	1480	1390	1400	1348	1385
IV	1378	1500	1390	1410	1338	1377
Ice Cap	1185	1275	1240	1250	1173	1197
Cirque Mean	1380	1489	1393	1409	1349	1385

Previous work in the circum-Caribbean region suggests the present day 0°C isotherm and ELA for Mexico, Costa Rica and Venezuela is $\sim 4900 \pm 200$ m, which provides a rough estimate for the entire Central American region (Lachniet and Seltzer, 2002; Lachniet and Vázquez-Selem, 2005). This estimates falls within the range of Kageyama et al., (2005) who modeled temperature lapse rates and the 0°C isotherm in the tropical

atmosphere. For the Guatemalan field site (91.5°W, 15.5°N) modeling efforts suggest a present day ELA of 4800 to 5000 m which is similar to the circum-Caribbean estimate. For this research the circum-Caribbean present day ELA of 4900 ± 200 m will be used for Δ ELA calculations. The Δ ELAs for the plateau ice cap and cirque glaciers are given in table 3 which estimates the amount of $ELA_{BR=2}$ to be $\sim 1200 \pm 200$ m for the ice cap and $\sim 1400 \pm 200$ m for the cirques which is consistent with previously published values from Lachniet and Vázquez-Selem, (2005) of 1300 to 1500 m for the entire circum-Caribbean region.

Calculating the LLGM paleotemperature of the plateau and Montaña San Juan from THAR, AAR and AABR ELA estimates is done by multiplying the present day temperature lapse rate and the Δ ELA. Present day temperature lapse rates for Guatemala were calculated to be $-5.3^\circ\text{C km}^{-1}$ from the INSUVIMEH , (2006) climate data which is similar to the NCEP estimated temperature lapse rate presented in Kageyama et al., (2005) who reports it to be -5.25 to $-5.5^\circ\text{C km}^{-1}$ at $\sim 15^\circ\text{N}$. An assessment of the northern Guatemalan highlands temperature depression from present (ΔT) was made using the $\Delta ELA_{BR=2}$ for the ice cap, which yields:

$$(-5.3^\circ\text{C km}^{-1})(1197\text{m}) = \Delta T = -6.3^\circ\text{C}$$

An average for all 5 cirques yields:

$$(-5.3^\circ\text{C km}^{-1})(1385 \text{ m}) = \Delta T = -7.3^\circ\text{C}$$

There is a distinct $\sim 1^\circ\text{C}$ difference between the two regions, evident by the data in Table 4. The 200-m uncertainty of the present day Central American ELA (4900 ± 200 m) translates into a $\pm 1.1^\circ\text{C}$ uncertainty in the temperature estimate based on the lapse rate of $-5.3^\circ\text{C km}^{-1}$. The full range of ΔT is given in table 4 for each of the table 3 Δ ELA

estimates. A clear $\sim 1^{\circ}\text{C}$ difference is evident by the values of ΔT between the north facing cirque glaciers and the small plateau ice cap. The estimates show good internal consistency between the different reconstruction methods; a range of ΔT is only -6.9°C to -8.2°C for the cirques and -6.2°C to -6.8°C for the plateau ice cap. Both of these ranges also fall within or near the $\pm 1.1^{\circ}\text{C}$ uncertainty that is introduced by the present day ELA error of $\pm 200\text{m}$.

Table 4. Table of specific temperature depression values (ΔT) ($\pm 1.1^{\circ}\text{C}$) for the plateau region and the Montaña San Juan showing two estimates of the THAR, AAR and the AABR methods used in this analysis.

Glacier	THAR = 0.7	THAR = 0.5	AAR = 0.6	AAR = 0.65	BR = 1.0	BR = 2.0
I	-7.1	-7.5	-7.2	-7.2	-6.9	-7.0
II	-7.5	-8.2	-7.6	-7.7	-7.5	-7.7
III	-7.3	-7.8	-7.4	-7.4	-7.1	-7.3
IV	-7.3	-8.0	-7.4	-7.5	-7.1	-7.3
Ice Cap	-6.3	-6.8	-6.6	-6.6	-6.2	-6.3
Cirque Mean	-7.3	-7.9	-7.4	-7.5	-7.1	-7.3

Glacier Modeling Estimates

The GIS glacier model of Plummer and Phillips, (2003) provides a quantitative way to reconstruct paleoclimate based on modeling mass balance of a previously glaciated region. This procedure has been used with some success in mid-latitude and tropical paleoglacier and paleoclimate reconstructions (i.e., Laabs et al., 2006) although never before used to model a tropical ice cap. Modeling the specific mass balance of the plateau and Montaña San Juan regions provided a comparison of the temperature estimates made

via the Δ ELA calculated from the THAR, AAR and AABR methods. Target ELAs for the ice cap were taken from the estimates of the previously published Guatemalan LLGM ELA of 3650 m (Lachniet and Vázquez-Selem, 2005) while for the cirque glaciers, the estimate was made from the maximum elevation of lateral moraines (MELM) which gives an average target ELA of ~3500 m. Any estimate of the GIS-calculated LLGM ELA that was within ± 100 m of the target ELAs was considered a suitable paleoclimate representation; those values are given in table 5. Since there are multiple combinations of temperature depression and precipitation totals that would infer estimates close to the target ELAs, the model provides a range of the Guatemalan highland LLGM climate. From the GIS model a LLGM temperature depression is estimated at -4.5°C for the plateau and -4.75 to -5.0°C when combined with precipitation totals that are equal (100%) to present day (Fig. 14). The graph shows an apparent dominant control of temperature on glaciation vs. precipitation changes. Changes in precipitation totals do affect the temperature depression values, so a range of realistic precipitation totals was created based on INSIVUMEH, (2006) climate data. The 1990 – 2003 Todos Santos yearly precipitation records show no precipitation totals that are below 50% and above 30% of the average for the entire record. The GIS model was therefore run with precipitation totals that are below 150% and above 50% of present day totals.

Mass balance gradients were calculated from the model output GIS data in order to check the model's ability to realistically portray tropical balance ratios. Four model runs that fell within the cirque target ELA were used to determine the average mass balance gradient of the Montaña San Juan region. The cirque glaciers place a tight constraint on the specific mass balance vs. elevation estimates due to the small extent of the ice. The

plateau region was too broad to provide an accurate average for the entire ice cap. The model output also revealed there was a prevalent north-northwest dipping gradient of the 0 mass balance line making a generalization of the plateau ice cap ELA difficult. The output data provides an estimate of the mass balance at some elevation; in order to constrain the mass balance gradient for the cirque glaciers, data was taken for each 50 m

Table 5. A table of the LLGM ice cap (IC) and cirque average (C) equilibrium line altitude (ELA) estimates based on the modeled variations in temperature (T) and precipitation (amount of present day annual totals) (P). Bold ELA estimates represent the values that were within 100m of the target ELAs of 3650m for the ice cap and the cirque glaciers of 3500m.

T (°C)	P	IC ELA	C ELA (avg)
-6.3	50%	3600	3620
-6.0	60%	3540	3500
-5.8	60%	3580	3560
-5.5	60%	3620	3620
-5.5	75%	3540	3540
-5.0	75%	3620	3620
-5.0	80%	3600	3620
-4.8	100%	<3400	3540
-4.8	80%	<3400	3520
-4.5	100%	3640	3640
-4.5	80%	3700	3680
-4.0	125%	3700	3700

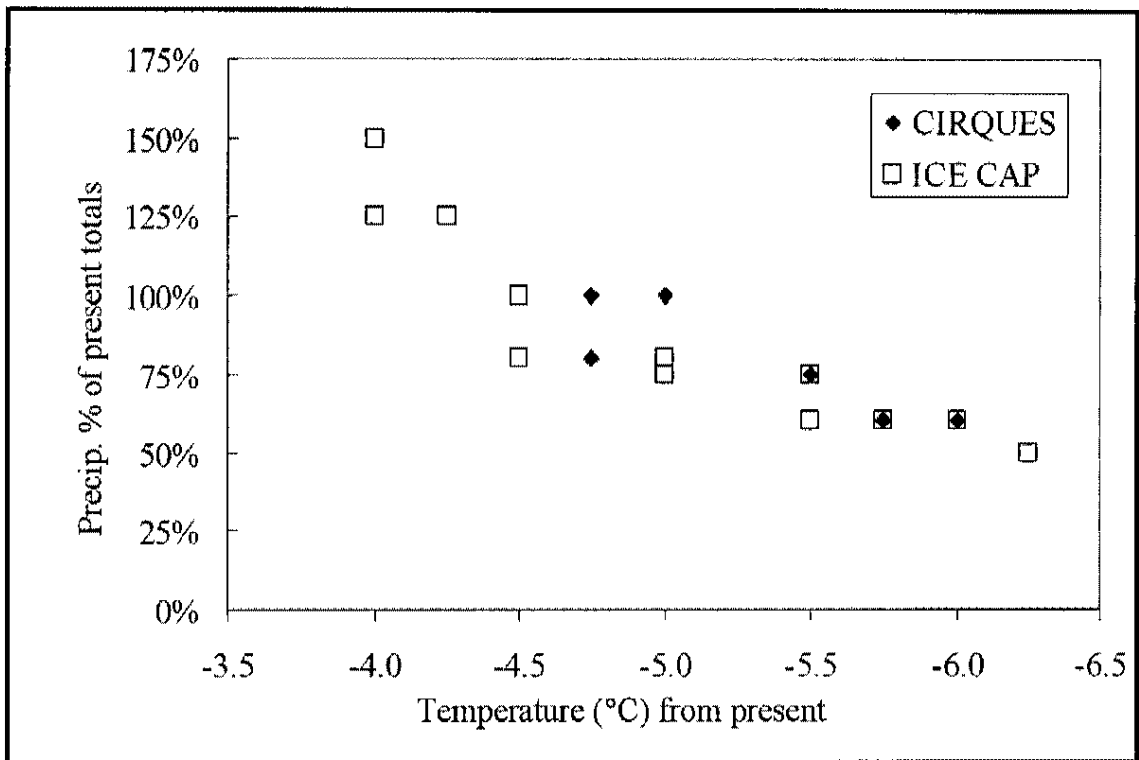


Figure 14. Climate-space diagram showing temperature and precipitation combinations for modeled ELAs that were similar to the ice cap target ELA of 3650 m and the cirque target ELA of 3500 m. Estimates of the plateau (boxes) and Montaña San Juan (diamonds) LLGM climate shows that temperature changes are the dominant control for sustaining glacier ice in this region. Ranges in the precipitation totals for a given temperature are due to slightly different ELAs relative to the target ELA, typically not to exceed 50m.

contour from 3150 to 3700 m. The four mass balance gradients were plotted and the mean taken to determine that the $BR = \sim 1.5$ for the cirque glaciers of the Montaña San Juan (Fig. 12). This estimate falls below previously published tropical BR values (i.e., $BR = 2-4$) although is in line with a $BR = 1-2$ that was found for outer-tropical regions by Osmaston, (2005). It has been shown that the aspect, shading and debris cover can significantly decrease the BR, both by increased accumulation due to shading or decreased ablation due to debris cover on the glacier surface.

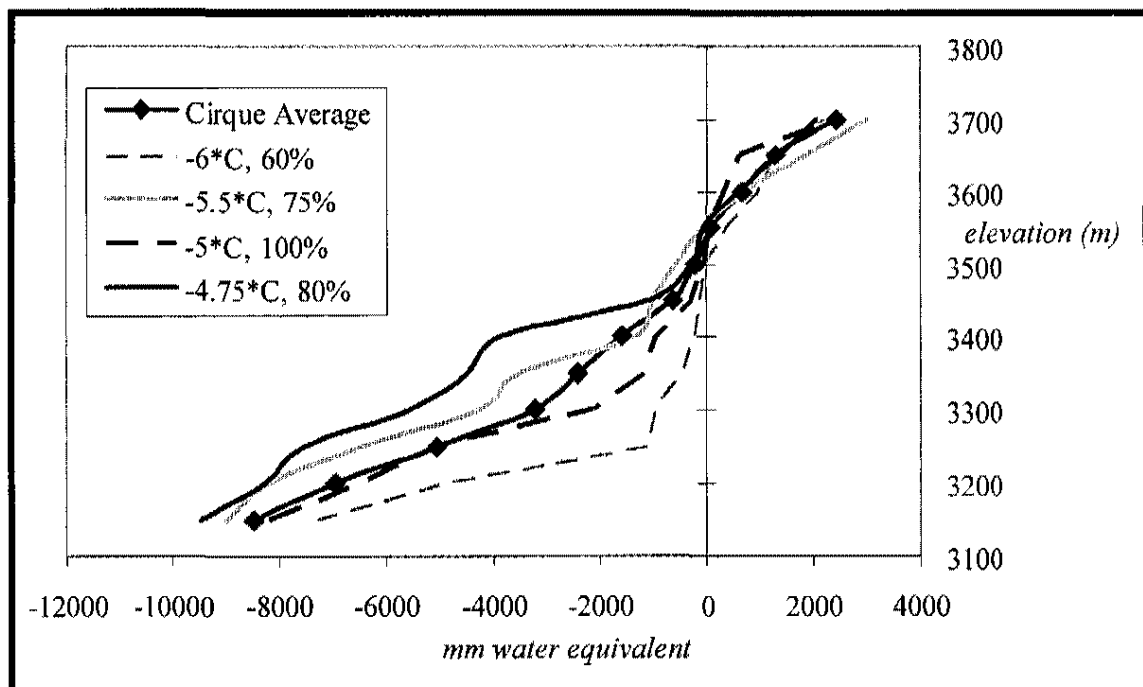


Figure 15. A plot of four mass balance gradients and the mean for the reconstructed cirque glaciers of the Montaña San Juan. Data come from climate estimates (i.e., -5.5°C , 75% Precip.) that matched the target ELA of $\sim 3500\text{m}$ for the cirque glaciers. A balance ratio (BR) = ~ 1.5 was calculated which is consistent for some tropical locations.

The ice flow model is used to match maximum ice extent to the physical data mapped on the GIS. Based on numerous simulations the flow model failed to match the glacial geologic data for the ice cap by over and underestimating the ice extent. The physical data clearly demarcate the most eastern portions of the San Miguel, Tuizoche and Ninguitz Valleys maximum ice extent. The model results in ice limits that are far beyond the limits of the Ninguitz Valley moraines, but in the San Miguel Valley the model underestimated the advance (fig 16). The ice flow model does allow for some variation in the default values of ice velocity due to deformation and sliding which gives the flow model the ability to match regional geologic aspects. Uncertainties in describing glacier flow on an open plateau arose most likely due to the methods used in the Plummer and Phillips, (2003) model which have been set for regions with steep, narrow, glaciated valleys that constrain the ice (Refsnider et al., 2008; Laabs et al., 2006). The flow model, for even a small ice cap, cannot take into account a potential spatial precipitation gradient that could distribute precipitation unevenly across the accumulation area or a change in the majority wind direction which could cause drifting snow to accumulate in otherwise ice free areas, nor can it account for spatial variations in subglacial hydrology. Glacier ice flow was underestimated and overestimated using this same 2-D flow model for the western Uinta ice field in Utah, which was explained away by the inability of the climate portion of the model to correctly describe specific climate gradients across the field area (Refsnider et al., 2008).

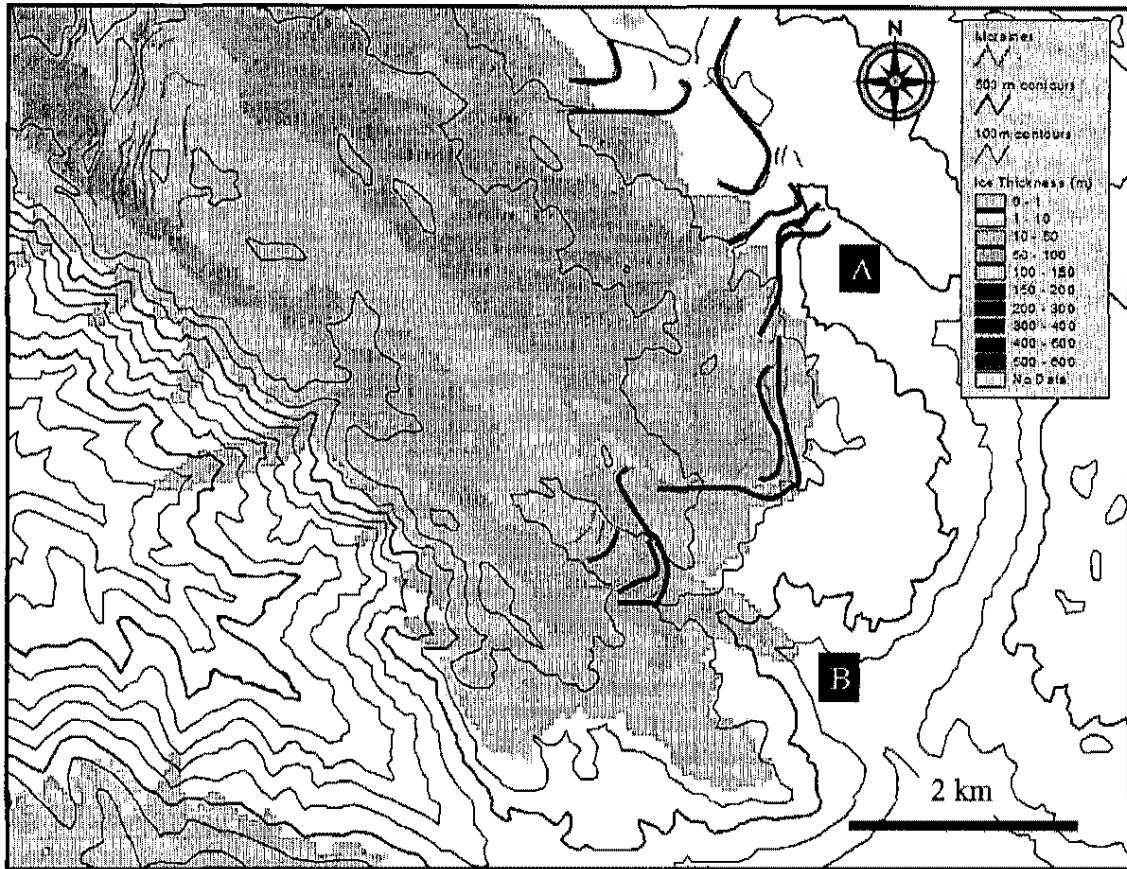


Figure 16. One version (-4.5°C and 100% of present day precipitation totals) of the modeled maximum ice extent and thickness for the eastern portion of the plateau ice cap, using the GIS flow model. The ice is clearly overextended past the largest moraine segments (black lines; smaller moraines are in grey) of the southern Ninguitz Valley (B) while the previously glaciated northern San Miguel Valley (A) remains ice free. The results indicate that the flow model was unable to accurately constrain ice dynamics on this tropical highland plateau.

CHAPTER 4

DISCUSSION

The study presented here utilized a combined approach to reconstructing the northern Guatemalan highlands maximum ice extent and subsequent LLGM ELA. This study also provides new insights into tropical highland paleoclimate that moves towards an improved understanding of the unresolved tropical temperature paradox. The prevalence of the glacial geomorphic evidence combined with computer-aided mapping and GIS modeling provides a robust reconstruction of the steady state maximum ice extent in this region. The tropical highland ΔT estimates presented here represent further evidence for more heavily depressed terrestrial temperatures than the average concurrent sea surface temperatures, while introducing new constraints on the Guatemalan highlands LLGM ELA and paleoclimate.

The Mayan Ice Cap and Cirque Glaciers

The Sierra de los Cuchumatanes supported a 35 to 40 km² plateau ice cap and a group of five north facing cirques along the Montaña San Juan (MSJ) ranging in length from 1 to 2 km. Mapping this region expands on previous work by Anderson (1969a, 1969b) and Hastenrath (1974) which provided a reconnaissance view of this region's diverse glacial geomorphology. There is noticeable evidence of glaciation in this region by the presence

of large terminal and lateral moraine segments, glacially scoured bedrock, plucked surfaces, subglacial till and proglacial sediment deposits. Field evidence suggests more extensive glacial ice extent than suggested by previous publications. The THAR, AAR and AABR methods were employed to determine the LLGM ELA after extensive glacial geologic mapping was completed. The AABR calculated LLGM $ELA_{BR=2.0}$ is 3703 m for the plateau ice cap and a cirque average LLGM $ELA_{BR=2.0}$ of 3515 m. These estimates are in good agreement with the circum-Caribbean mean $ELA_{BR=1.8}$ of 3839 ± 370 m which was reported in Lachniet and Vázquez-Selem, (2005). The small altitudinal range of the plateau (3470 to 3830 m) and MSJ (~3000 to 3700 m) glacial evidence presents further constraints on these northern Guatemalan highlands LLGM ELA estimates. The present day ELA for Guatemala is taken from the circum-Caribbean average of 4900 ± 200 m which yields a ΔELA to be $\sim 1200 \pm 200$ m for the plateau and $\sim 1380 \pm 200$ m for the cirque glaciers of the Montaña San Juan. Published ΔELA estimates from Mexico (~1500 m), Costa Rica (~1500 m) and Venezuela (~1300 m) (i.e., Lachniet and Vázquez-Selem, 2005, Stansell et al., 2007) provide further correlation to the values presented here.

The method of calculating a temperature depression based solely on the ΔELA depends on including 1) a reliable regional temperature lapse rate and 2) the present day atmospheric 0°C isotherm and 3) adequate glacial evidence that allows for a comprehensive estimate of the maximum ice extent (Benn et al., 2005). The temperature lapse rate varies slightly in the tropics ranging from -5.1 to $-6.0^\circ\text{C km}^{-1}$ (Kageyama et al., 2005; Mark et al., 2005) most likely due to minor differences in humidity which can alter the lapse rate estimate. This range is in good agreement with the calculated Guatemalan atmospheric lapse rate of $-5.3^\circ\text{C/km}^{-1}$ used in this project. When combined with the well

recognized present day 0°C isotherm estimate of 4900 ± 200m for this region (Lachniet and Vázquez-Selem, 2005; Vázquez-Selem and Heine, 2004; Lachniet and Seltzer, 2002) yields a northern Guatemalan highland LLGM temperatures which were -6.4 ± 1.1°C (plateau) and as much as -7.4 ± 1.1°C (Montaña San Juan) from present day.

Although no chronology was established, photographic evidence provided constraints on ice dynamics and an apparent correlation between the morphology (i.e., crest shape, size) of the Mexican LLGM (MIS 2; ~18 to 21 ka) moraines and the purported LLGM moraines of the northern Guatemalan highlands (Vázquez-Selem, pers. comm., 2006). Field observations suggest that the high weathering rate of the limestone bedrock, along with the prevalence of well formed glacial geomorphology, places the timing of maximum glacial advance during the global LGM ~16 to 24 ka. The Guatemalan moraines that correlated to the Mexican moraines show defined crests along with pronounced peaks that would not have been observed if glaciation occurred during the penultimate marine isotope stage (MIS) 6 (~125 ka) previous glacial maximum. These moraines and glacial evidence would be far more weathered if glaciation had occurred during the previous MIS 6 glaciations. There are large, muted moraine segments that are positioned up valley from the prominent eastern San Miguel Valley moraines, but it is unclear at this time what glaciation or ice advance period they represent.

Paleotemperature Discrepancies

The Plummer and Phillips (2003) model provides a new method for reconstructing former ice extents, along with providing estimates of both paleotemperature and paleoprecipitation. The modeled range of ΔT (-4.0 to -6.3°C from present) estimates for

the entire Sierra de los Cuchumatanes was noticeably higher than the -7.4 to -6.4°C ΔT calculated from the physical data. Modeling the Sierra de los Cuchumatanes plateau region and nearby Montaña San Juan cannot be easily grouped together with equal affects of glacier aspect and climate.

There are many factors that could account for the discrepancy between the temperature estimates that were based on the physical data and those estimated via the GIS model. Uncertainties associated with the modeling efforts started with the lack of any net annual snow accumulation that could be used to calibrate the model to present day climate. Plummer and Phillips (2003) modeled present day small perennial snow fields that were mapped on topographic maps before the paleo-glacier GIS modeling began. Similarly the climate data, which are the primary input for the glacier model, were valley specific for the reconstructed glaciers reported in Plummer and Phillips (2003). For this research the closest available monthly climate data came from Todos Santos (2480 m), a small town situated in a large valley 1220 m lower in elevation than the ~ 3700 m average of the plateau and Montaña San Juan field areas. Several key climate factors that affect a glaciers annual mass balance were unresolved when using this model. From the present climate data an apparent change in the environmental lapse rate with elevation remains uncertain, especially in the highland regions above 2000m. Other climate parameters such as increased windiness, which causes snow drifting, and changes in the insolation budget on the glacier surface due to debris cover were unconstrained.

Similarly, in the tropics a common daily occurrence is mid-afternoon precipitation combined with increased cloudiness due to the effects of convection and evaporation. This increase in cloudiness during the afternoon hours, or the warmest part of the day,

has been shown to favor a westward aspect of glaciers in the tropics by reducing the available incoming solar radiation to western slopes (Benn, 2006). The glacier modeling did provide estimates of mass balance vs. elevation which allowed for a regional balance ratio to be calculated. Mass balance data from the Montaña San Juan cirque glaciers gives a representative balance ratio of ~1.5 which is slightly below typical values found in tropical regions of 1.7 to 4.0 (Mark et al., 2005; Kaser and Osmaston, 2002) although further modeling could constrain this regional value.

Highland Glacier Dynamics

Glacier flow modeling efforts were unsuccessful in reproducing maximum ice extents that matched the physical evidence, although the model did provide valuable insight into ice accumulation and flow characteristics across the plateau surface and nearby Montaña San Juan. The glacial evidence observed on the plateau corresponds to a history of multiple glacial advances and in some cases a slow retreat of a small ice cap. This is made apparent by the large (15 to 20 m) double crested terminal moraines of the eastern Tuizoche and San Miguel Valleys along with groups of nested muted recessional moraines mapped along the Colinas Planas to the west. Local topography had a large influence on ice dynamics by providing a general dip direction of the plateau region to the northeast and the east-west trending ridgeline of the Montaña San Juan. The largest (i.e. highest relief) moraine segments are concentrated along the eastern edge of the plateau region which corresponds to the general dip of the plateau. Although little evidence was observed on the southern edge of the plateau, avalanching could have influenced the minimum elevation ice would flow down valley, which is common in

steep glaciated regions (Benn and Evans, 1998). Similarly, there were certain smaller valleys along the southern edge that revealed no observable glacial evidence, but that the GIS model would specifically utilize as an outlet for ice cap glacier tongues. The highest point on the plateau region was not directly observed, so it is unclear if these areas were completely glaciated or existed as nunataks during the Guatemalan LLGM. Further mapping efforts that could describe the location-specific glacial geology and the full extent of glacial evidence may improve the glacier reconstruction.

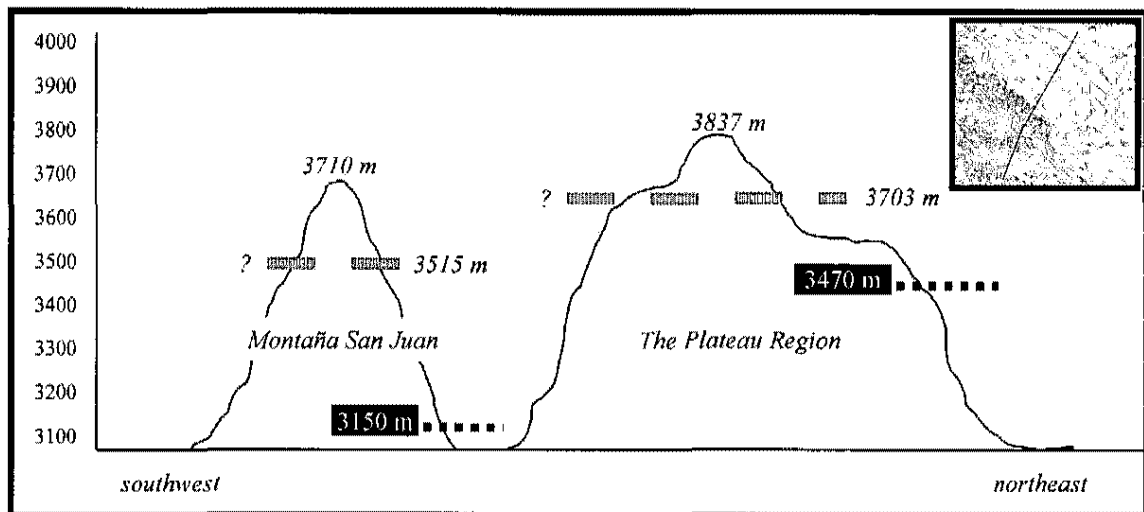


Figure 17. Topographic profile of the plateau region and Montaña San Juan (see inset) showing the location of the LLGM ELA_{BR=2} (grey dashed lines) along with the lowest limit of glacial evidence (black dotted line). For the plateau the difference between the highest glaciated peak and lowest ice positions is ~370m while for the Montaña San Juan the value reaches almost 600m. There is a distinct difference in the lowest ice limits between the two regions, although the affect of aspect on glaciation is more apparent when viewing the Montaña San Juan.

Shading, slope and aspect have been shown to influence the microclimate around a glaciers surface which in turn alters glacier dynamics (Evans, 2006). A global review of present glaciers reveals there is a preferred pole ward orientation which is more prevalent in the mid-latitudes but still common in the tropics (Evans, 2006). The effect of aspect on Guatemalan glaciation is apparent by the prevalence of perennial ice that is situated at much lower elevations along the north to northeast facing slopes and the dominance of ice along the northern lobes of the Montaña San Juan (Fig. 17). It is unclear at this time of the effects of asymmetry of the Montaña San Juan ridge, which suggests that the more gentle northern slopes could have allowed for greater accumulation rates. Whatever the primary influence on glaciation was during the LLGM, the importance of shading and the glaciers solar radiation budget on the glaciers mass balance must be considered (Evans, 2006). The effects of aspect allow for changes in the solar radiation budget to alter glacier dynamics, where a minimum occurs either due to shading or a loss of heat transfer when winds are blocked or subdued (Evans, 2006; Plummer and Philips, 2003; Benn and Evans, 1998). Aspect had minor effect on the plateau ice cap since the amount of solar radiation was similar across the plateau although in some instances, like the northern slopes of high ridges and the eastern sections of the San Miguel, Ninguitz and Tuizoche valleys, shading and insolation minimums could have occurred.

Subsole deformation of the basal sediments and basal sliding account for a large part of a glacier's forward movement, and varies via the pore water pressure at the base of the glacier (Benn and Evens, 1998). If the predominately carbonate/limestone rich bedrock was well drained (i.e. subglacial sinking streams) and reduced the amount of water available at the base, sliding would be diminished due to the lack of high porewater

pressures between the ice and bedrock along with a reduction of available water within the deforming sediments at the base of the glacier. One area of subsurface deformation was observed in a well dug into the terminal glacial sediments in Ninguitz Valley, which indicates the ice moved via some deforming sediments and not entirely by basal sliding. Since the GIS model allows for only a broad estimate of the glaciers basal sliding dynamics, these small scale differences in the subsurface that could affect the flow model remain unconstrained at this time. The spatial distribution of water plays a critical role in the movement of the glacier along the base; studies have shown that there is enhanced movement of glacier ice during times of increased basal water pressure (Benn and Evens, 1998). If the basal water is redirected, through dissolution features or subsurface drainage, sliding amounts would be disproportional across the basal surface of the glacier. Important factors that influence glacier sliding like adhesion of ice to the bed surface due to freezing or the amount of bed roughness may have been affected by the presence of easily eroded limestone due to its lower density (Benn and Evens, 1998).

Future Work

A large portion of the field work included sampling boulders resting along moraine crests for cosmogenic exposure age determination. Fifteen boulders were sampled from the apparent terminal moraines of the eastern plateau region. At this time funding is not currently available for the ^{36}Cl dating, so it was not completed for this study. If these samples could be analyzed using the accumulation of cosmogenic ^{36}Cl in the limestone (CaCO_3) an absolute chronology of the Guatemalan highlands LLGM could be made.

The retreat of the ice cap resulted in the formation of small lakes set behind the plateau region moraines (Fig. 18), trapping glacial sediments during the ice retreat. If

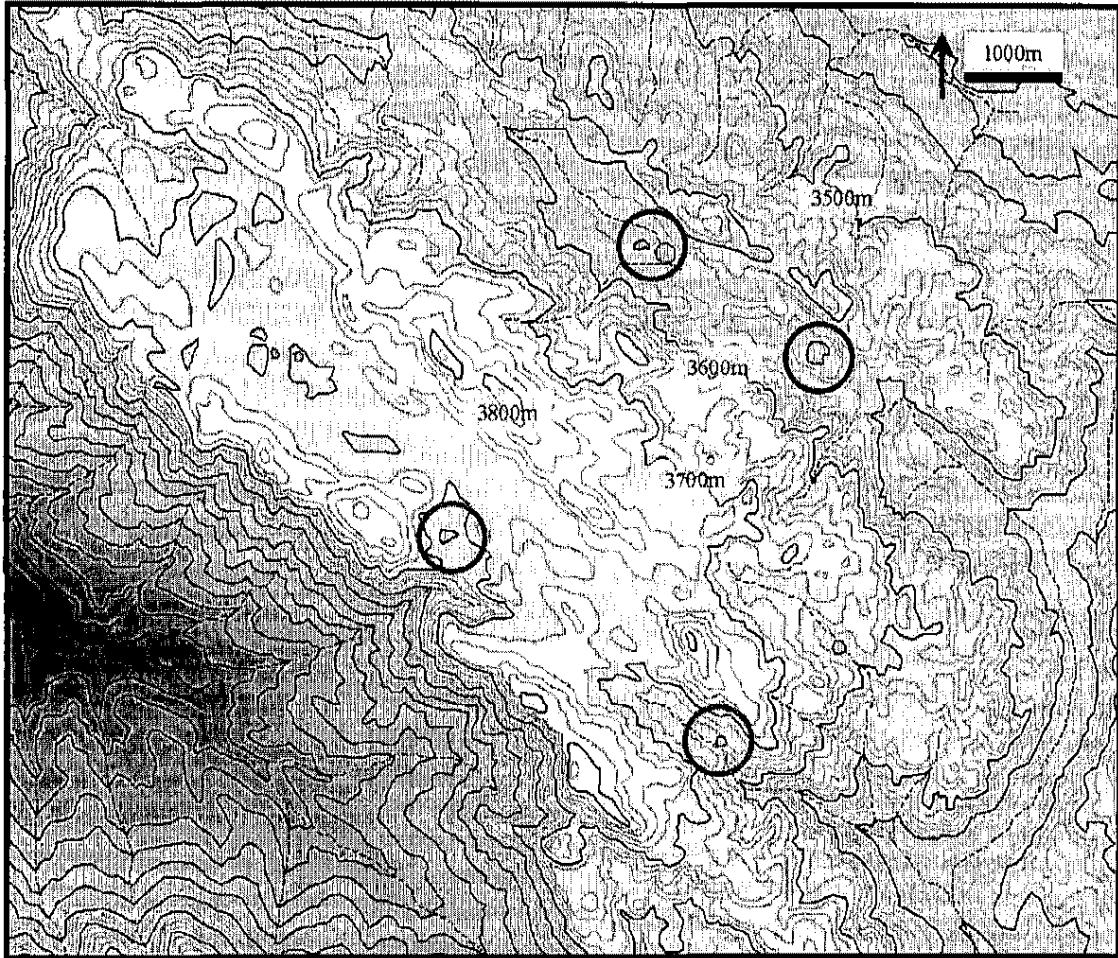


Figure 18. DEM of the plateau region showing the location of ephemeral moraine dammed lakes (circled in red). During field work these lakes were empty (March) but if cored could provide samples of organic material for ^{14}C dating; this would allow some estimate of the minimum age of deglaciation for the plateau region.

suitable organic material can be discovered in core samples, combined with interpretations of sediment facies, a minimum age of deglaciation can be estimated. At least four ephemeral moraine dammed lakes may provide suitable organic material used in building a ^{14}C chronology. Two of the lakes were visited during the March 2006 field work and were observed to be completely dry. The lakes are filled during the wet season (Geronimo Pablo Ramírez pers. comm., 2006) and are emptied most likely through subsurface drainage in the limestone bedrock. Based on the location of the lakes relative to the mapped moraines there may be evidence of the timing of deglaciation for at least two different large glacial pulses, one during the maximum extent and a smaller advance that only covered the interior of the plateau region.

Using basal shear stress calculations to evaluate ice thickness allowed for some small outlet glaciers to be mapped, but with no apparent glacial evidence. Visiting these specific valleys could reveal more evidence for the determination of maximum ice extent. Furthermore, mapping all of the moraines via GPS with altitude, relief and length measurements would provide further confirmation between the different moraine groups based on more specific spatial references. Only the furthest extents of glacial moraines were mapped with GPS, as a result mapping the detailed location of smaller moraines would alter the present cirque and ice cap reconstruction. For the cirques of the Montaña San Juan there was no direct field evidence made. The mapped moraines were taken from aerial photographs with a large degree of shading hiding possible small scale or muted glacial deposits. Small scale deposits in the cirques may have eluded the aerial photograph scale and would warrant a more comprehensive visit to the northern Guatemalan highlands field area.

REFERENCES

- Aguilar, E., Peterson, T.C., Obando, P.R., Frutos, R., Retana, J.A., Solera, M., Soley, J.f, García, I.G., Araujo, R.M., Santos, A.R., Valle, V.E., Brunet, M., Aguilar, L., Álvarez, L., Bautista, M., Castañón, C., Herrera, L., Ruano, E., Sinay, J.J., Sánchez, E., Oviedo, G.I.H., Obed, F., Salgado, J.E., Vázquez, J.L., Baca, M., Gutiérrez, M., Centella, C., Espinosa, J., Martínez, D., Olmedo, B., Espinoza, C.E.O., Núñez, R., Haylock, M., Benavides, H., and Mayorga, R., 2005, Changes in precipitation and temperature extremes in Central America and northern South America, 1961-2003: *Journal of Geophysical Research D: Atmospheres*, v. 110, p. 1-15.
- Anderson, T.H., 1969a, First evidence for glaciation in Sierra Los Cuchumatanes Range, northwestern Guatemala. Abstracts of papers submitted for the meeting in Dallas, Texas, March 29–31, 1968. *Geological Society of America Special Paper 121*, p. 387.
- Anderson, T.H., 1969b, Geology of the San Sebastian Huehuetenango quadrangle, Guatemala. Ph.D. Dissertation, University of Texas, Austin.
- Anselmetti, F.S., Ariztegui, D., Hodell, D.A., Hillesheim, M.B., Brenner, M., Gilli, A., McKenzie, J.A. and Mueller, A.D., 2006, Late Quaternary climate-induced lake level variations in Lake Petén Itzá, Guatemala, inferred from seismic stratigraphic analysis, *Paleogeography, Paleoclimatology, Paleoecology*, v. 230 (1-2), p. 52-69.
- Benn, D.I. and Evans, D.J., 1998, *Glaciers and Glaciation*, John Wiley and Sons, New York, pp.734.
- Benn, D.I. and Lehmkuhl, F., 2000, Mass balance and equilibrium-line altitudes of glaciers in high-mountain environments. *Quaternary International*, v. 65-66, p. 15-29.
- Benn, D.I., Gemmell, A.M.D., 1997. Calculating equilibrium-line altitudes of former glaciers by the balance ratio method: a new computer spreadsheet. *Glacial Geology and Geomorphology*. Web page: <http://ggg.qub.ac.uk/ggg>.
- Benn, D.I., Owen, L.A., Osmaston, H.A., Seltzer, G.O., Porter, S., Mark, B., 2005, Reconstruction of equilibrium line altitudes for tropical and subtropical glaciers. *Quaternary International*, v. 138-139, p. 8-21.

- Blard, P.-H., Lavé, J., Pik, R., Wagnon, P., Bourlès, D., 2007, Persistence of full glacial conditions in the central Pacific until 15,000 years ago, *Nature*, v. 449 (7162), p. 591-594.
- Bolstad, P., 2005, *GIS Fundamentals*; 2nd edition, Eider Press, Minnesota, pp. 543
- Bundschuh, J., Alvarado, G.E., eds., 2007, *Central America: Geology, Resources and Hazards*, Taylor and Francis Ltd, London, 1436 p.
- CLIMAP Project Members, 1976, The surface of the ice-age Earth, *Science*, v. 191(4232), p. 1131-1137.
- CLIMAP Project Members, 1981, Seasonal Reconstruction of the Earth's Surface at the Last Glacial Maximum, *Geological Society of America Map and Chart Series*, no. MC-36.
- Evans, I.S., 2006, Local Aspect and asymmetry of mountain glaciation: A global survey of consistency of favored directions for glacier numbers and altitudes, *Geomorphology*, v. 73, p. 166-184.
- Furbish, D.J., Andrews, J.T., 1984, The use of hypsometry to indicate long-term stability and response of valley glaciers to changes in mass transfer, *Journal of Glaciology*, v. 30, p. 199–211.
- Guilderson, T.P., Fairbanks, R.G., Rubenstone, J.L., 1994, Tropical temperature variations since 20,000 years ago: Modulating interhemispheric climate change. *Science*, v. 263 (5147), p. 663-665.
- Guilderson, T.P., Fairbanks, R.G., Rubenstone, J.L., 2001, Tropical Atlantic coral oxygen isotopes: Glacial-interglacial sea surface temperatures and climate change, *Marine Geology*, v. 172 (1-2), p. 75-89.
- Hastenrath, S., 1974, Spuren pleistozäner Vereisung in den Altos de Cuchumatanes, Guatemala, *Eiszeitalter und Gegenwart*, v. 25, p. 25–34.
- Hillesheim, M.B., Hodell, D.A., Leyden, B.W., Brenner, M., Curtis, J.H., Anselmetti, F.S., Ariztegui, D., Buck, D.G., Guilderson, T.P., Rosenmeier, M.F., Schnurrenberger, D.W., 2005, Climate change in lowland Central America during the late deglacial and early Holocene, *Journal of Quaternary Science*, v. 20 (4), p. 363-376.
- Hodell, D.A., Anselmetti, F.S., Ariztegui, D., Brenner, M., Curtis, J.H., Gilli, A., Grzesik, D.A., Guilderson, T.J., Müller, A.D., Bush, M.B., Correa-Metrio, A., Escobar, J., Kutterolf, S., An 85-ka record of climate change in lowland Central America. *Quaternary Science Reviews*, in press.

Hodell, D.A., Brenner, M., Curtis, J.H., 2007, Climate and cultural history of the Northeastern Yucatan Peninsula, Quintana Roo, Mexico, *Climatic Change*, v. 83 (1-2), p. 215-240.

Hodell, D.A., Curtis, J.H., Jones, G.A., Higuera-Gundy, A., Brenner, M., Binford, M.W., Dorsey, K.T., 1991, Reconstruction of Caribbean climate change over the past 10,500 years, *Nature*, v. 352 (6338), p. 790-793

Hostetler, S.W., Clark, P.U., 2000, Tropical climate at the last glacial maximum inferred from glacier mass-balance modeling, *Science*, v. 290 (5497), p. 1747-1750.

INSIVUMEH, accessed, 2006, <http://www.insivumeh.gob.gt/>, Instituto Nacional de Sismologia, Vulcanologia, Meteorologia y Hidrologia, 7a Ave, Zona 13, Guatemala Ciudad, Guatemala.

Islebe, G. and Hooghiemstra, H., 1997, Vegetation and climate history of montane Costa Rica since the last glacial. *Quaternary Science Reviews*, v. 16 (6), p. 589-604.

Kageyama, M., Harrison, S.P. and Abe-Ouchi, A., 2005, The depression of tropical snowlines at the last glacial maximum: What can we learn from climate model experiments? *Quaternary International*, v. 138-139, p. 202-219.

Kaser, G., and Osmaston, H., 2002, *Tropical Glaciers*, Cambridge University Press, Cambridge, 207 p.

Laabs, B.J., Plummer, M.A., Mickelson, D.M., 2006, Climate during the last glacial maximum in the Wasatch and southern Uinta Mountains inferred from glacier modeling, *Geomorphology*, v. 75 (3-4), p. 300-317.

Lachniet, M.S., Seltzer, G.O., 2002, Late Quaternary glaciation of Costa Rica. *Geological Society of America Bulletin* v. 114, p. 547-558, Correction in *GSA Bulletin* v. 114, p. 922.

Lachniet, M.S., Vázquez – Selem, L., 2005, Last glacial maximum equilibrium line altitudes in the circum-Caribbean (Mexico, Guatemala, Costa Rica, Columbia and Venezuela), *Quaternary International*, v. 138- 139, p. 129 – 144.

Lea, D.W., Pak, D.K. and Spero, H.J., 2000, Climate impact of late Quaternary Equatorial Pacific sea surface temperature variations, *Science*, v. 289 (5485), p. 1719-1724.

Lea, D.W., Pak, D.K., Peterson, L.C., Hughen, K.A., 2003, Synchronicity of tropical and high-latitude Atlantic temperatures over the last glacial termination, *Science*, v. 301 (5638), p. 1361-1364.

Leduc, G., Vidal, L., Tachikawa, K., Rostek, F., Sonzogni, C., Beaufort, L., Bard, E., 2007, Moisture transport across Central America as a positive feedback on abrupt climatic changes, *Nature*, v. 445 (7130), p. 908-911.

Leyden, B.W., 2002, Pollen evidence for climatic variability and cultural disturbance in the Maya Lowlands, *Ancient Mesoamerica*, v. 13, p. 85-101.

Leyden, B.W., Brenner, M., Hodell, D.A., Curtis, J.H., 1994, Orbital and internal forcing of climate on the Yucatan Peninsula for the past ca. 36 ka, *Palaeogeography, Palaeoclimatology, Palaeoecology*, v. 109 (2-4), p. 193-210.

Leyden, B.W., 1995, Evidence of the Younger Dryas in Central America, *Quaternary Science Reviews*, v. 14 (9), p. 833-839.

Magaña, V.O., Amador, J.A., Medina, S., 1999, The midsummer drought over Mexico and Central America, *Journal of Climate*, v. 12 (6), p. 1577-1588.

Magaña, V.O., Vázquez, J.L., Pérez, J.L., Pérez, J.B., 2003, Impact of El Niño on precipitation in Mexico, *Geofísica Internacional*, v. 42 (3), p. 313-330.

Mark, B.G., Harrison, S.P., Spessa, A., New, M., Evans, D.J.A., Helmens, K.F., 2005, Tropical snowline changes at the Last Glacial Maximum: a global assessment, *Quaternary International*, v. 138-139, p.

Mark, B.G., Helmens, K.F., 2005, Reconstruction of glacier equilibrium-line altitudes for the Last Glacial Maximum on the High Plain of Bogotá, Eastern Cordillera, Colombia: Climatic and topographic implications, *Journal of Quaternary Science*, v. 20 (7-8), p. 789-800.

Marshall, J.S., 2006, *Geomorphology and Physiographic Provinces of Central America*: in Bundschuh, J. and Alvarado, G., eds., *Central America: Geology, Resources, and Hazards*, Taylor and Francis, London, p. 75-122.

Metcalf, S., Say, A., Black, S., McCulloch, R., O'Hara, S., 2002, Wet conditions during the last glaciation in the Chihuahuan Desert, Alta Babilcora Basin, Mexico, *Quaternary Research*, v. 57 (1), p. 91-101.

Mix, A.C., Morey, A.E., Pisias, N.G., Hostetler, S.W., 1999, Foraminiferal faunal estimates of paleotemperature: Circumventing the no-analog problem yields cool ice age tropics, *Paleoceanography*, v. 14 (3), p. 350-359.

Napieralski, J., Harbor, J., Li, Y., 2007, Glacial geomorphology and geographic information systems, *Earth-Science Reviews*, v. 85 (1-2), p. 1-22.

Orvis, K.H., and Horn, S.P., 2000, Quaternary glaciers and climate on Cerro Chirripó, Costa Rica, *Quaternary Research*, v. 54, p. 24-37.

Osmaston, H., 2005, Estimates of glacier equilibrium line altitudes by the Area x Altitude, the Area x Altitude Balance Ratio and the Area x Altitude Balance Index methods and their validation, *Quaternary International*, v. 138 – 139, p. 22-31.

Paterson, W.S.B., 1981, *The physics of glaciers*, 2nd edition, Pergamon Press, 380 p.
Peterson, L.C., Haug, G.H., 2006, Variability in the mean latitude of the Atlantic Intertropical Convergence Zone as recorded by riverine input of sediments to the Cariaco Basin (Venezuela), *Palaeogeography, Palaeoclimatology, Palaeoecology*, v. 234 (1), p. 97-113.

Peterson, L.C., Haug, G.H., Murray, R.W., Yarincik, K.M., King, J.W., Bralower, T.J., Kameo, K., Rutherford, S.D., Pearce, R.B., 2000, Late Quaternary stratigraphy and sedimentation at Site 1002, Cariaco Basin (Venezuela), *Proceedings of the Ocean Drilling Program: Scientific Results*, v. 165, p 85-99.

Plummer, M.A., Phillips, F.M., 2003, A 2-D numerical model of snow/ice energy balance and ice flow for paleoclimatic interpretation off glacial geomorphic features. *Quaternary Science Reviews*, v. 22, p. 1389- 1406.

Porter, S.C., 2001, Snowline depression in the tropics during the last glaciation. *Quaternary Science Reviews*, v. 20 (10), p. 1067-1091.

Portig, W.H., 1965, Central American Rainfall, *Geographical Review*, Vol. 55, No. 1 (Jan., 1965), pp. 68-90

Refsnider, K.A., Laabs, B.J., Plummer, M.A., Mickelson, D.M., Singer, B.S., Caffee, M.W., 2008, Last glacial maximum climate inferences from cosmogenic dating and glacier modeling of the western Uinta ice field, Uinta Mountains, Utah, *Quaternary Research*, v. 69 (1), p. 130-144.

Rind, D., Peteet, D., 1985, Terrestrial conditions at the Last Glacial Maximum and CLIMAP sea-surface temperature estimates: are they consistent? *Quaternary Research*, v. 24, p. 1–22.

Schubert, C., 1974, Late Pleistocene Mérida glaciation, Venezuelan Andes, *Boreas*, v. 3, p. 147–151.

Schubert, C., Rinaldi, M., 1987, Nuevos datos sobre la cronología del estadio tardío de la glaciación Mérida, Andes Venezolanos. *Acta Científica Venezolana*, v. 38, p. 135–136.

Schultz, D.M., Bracken, W.E., Bosart, L.F., 1998, Planetary- and synoptic-scale signatures associated with Central American cold surges, *Monthly Weather Review*, v. 126 (1), p. 5-27.

- Schultz, D.M., Bracken, W.E., Bosart, L.F., Hakim, G.J., Bedrick, M.A., Dickinson, M.J., Tyle, K.R., 1997, The 1993 superstorm cold surge: Frontal structure, gap flow, and tropical impact, *Monthly Weather Review*, v. 125 (1), p. 5-39.
- Seltzer, G.O., 1992, Late Quaternary glaciation of the Cordillera Real, Bolivia, *Journal of Quaternary Science*, v. 7 (2), p. 87-98.
- Stansell, N.D., Polissar, P.J., Abbott, M.B., 2007. Last glacial maximum equilibrium-line altitude and paleo-temperature reconstructions for the Cordillera de Mérida, Venezuelan Andes, *Quaternary Research*, v. 67 (1), p. 115-127.
- Van Der Hammen, T., Hooghiemstra, H., 2003. Interglacial-glacial Fuquene-3 pollen record from Colombia: An Eemian to Holocene climate record, *Global and Planetary Change*, v. 36 (3), p. 181-199.
- Vázquez-Selem, L., and Phillips, F.M., 1998, Glacial chronology of Iztaccíhuatl volcano, central Mexico, based on cosmogenic ^{36}Cl exposure ages and tephrochronology [abs.]: in Program and Abstracts of the 15th Biennial Meeting, American Quaternary Association, AMQUA 1998, Northern Hemisphere-Southern Hemisphere Interconnections (5–7 September 1998; Puerto Vallarta, México), 174 p.
- Vázquez-Selem, L., Heine, K., 2004, Late Quaternary glaciation of Mexico. In: *Quaternary glaciations – Extent and Chronology Part III*, p. 233 – 243.
- White, S.E., 1981, Equilibrium line altitudes of Late Pleistocene and recent glaciers in Central Mexico, *Geografiska Annaler*, v. 63A, p. 241–249.
- White, S.E., 1986, Quaternary glacial stratigraphy and chronology of Mexico. *Quaternary Science Reviews*, v. 5, p. 201–205.
- White, S.E., 2002, Glaciers of Mexico. In: Williams, Jr., R.S., Ferrigno, J.G. (Eds.), *Satellite Image Atlas of the Glaciers of the World—Glaciers of North America*. US Geological Survey Professional Paper 1386-I. United States Government Printing Office, Washington, DC, p. J383–J405.
- White, S.E., Valastro Jr, S., 1984, Pleistocene glaciation of volcano Ajusco, central Mexico, and comparison with the standard Mexican glacial sequence, *Quaternary Research*, v. 21 (1), p. 21-35.

APPENDIX I

GIS MODEL CLIMATE DATA

Tables of climate data from station Todos Santos Cuchumatán (2480m) and station San Jose (~2 m) that was used to calculate the primary climate input for the Plummer and Phillips, (2003) GIS model. Data was collected from stored records in the Guatemalan Instituto Nacional de Sismología, Vulcanología, Meteorología e Hidrología (National Institute of Seismology, Volcanology, Meteorology and Hydrology) website at www.insivumeh.gob.gt/.

Todos Santos - Average monthly temperature (°C)						
	JAN	FEB	MAR	APR	MAY	JUN
<i>1990</i>	10.9	12.5	12.8	13.1	14.6	13.9
<i>1991</i>	11.5	12.1	15.0	15.0	16.6	15.2
<i>1992</i>	11.9	13.6	15.1	15.3	15.6	15.2
<i>1993</i>	11.4	13.4	14.1	15.7	15.3	14.9
<i>1994</i>	12.7	13.2	15.2	16.0	15.9	15.2
<i>1995</i>	13.2	15.1	14.6	15.0	15.0	15.0
<i>1996</i>	12.0	12.5	14.2	14.0	14.4	14.1
<i>1997</i>	12.7	15.0	14.2	15.0	14.3	14.0
<i>1998</i>	14.0	16.0	16.0	16.0	16.0	16.0
<i>1999</i>	14.0	14.2	15.6	16.0	15.4	16.0
<i>2000</i>	13.7	12.6	15.4	15.1	16.0	15.1
<i>2001</i>	14.7	14.6	14.6	15.4	15.0	16.0
<i>2002</i>	14.0	13.7	14.7	16.5	14.2	13.4
<i>2003</i>	10.8	13.1	13.9	15.7	15.2	15.4
AVG	12.68	13.69	14.67	15.27	15.25	14.96

Todos Santos - Average monthly temperature (°C)						
	JUL	AUG	SEP	OCT	NOV	DEC
<i>1990</i>	13.6	13.2	13.9	12.3	12.6	11.5
<i>1991</i>	14.8	14.3	13.9	13.0	11.4	11.2
<i>1992</i>	14.6	14.3	13.7	12.6	12.0	11.9
<i>1993</i>	14.8	13.9	14.0	13.9	13.5	13.0
<i>1994</i>	14.9	15.3	14.7	14.9	13.9	11.9
<i>1995</i>	14.7	14.6	14.2	14.6	14.1	13.0
<i>1996</i>	13.8	14.0	14.0	13.6	12.6	12.9
<i>1997</i>	13.0	14.0	14.0	14.0	15.0	15.0
<i>1998</i>	16.0	15.7	16.0	15.0	15.0	15.0
<i>1999</i>	14.0	14.0	14.5	14.0	12.5	13.1
<i>2000</i>	14.8	14.0	14.7	13.7	13.1	12.9
<i>2001</i>	15.0	15.0	15.0	14.0	13.0	14.0
<i>2002</i>	14.5	14.5	14.2	13.8	12.5	12.3
<i>2003</i>	14.7	14.4	14.9	13.8	13.2	11.0
AVG	14.51	14.37	14.41	13.80	13.17	12.76

Todos Santos - Average monthly precipitation totals (mm)						
	JAN	FEB	MAR	APR	MAY	JUN
<i>1990</i>	8.3	14.7	29.4	149.6	197.8	233.0
<i>1991</i>	0.0	0.0	0.0	60.2	270.9	245.0
<i>1992</i>	13.1	12.6	21.1	47.0	80.2	253.5
<i>1993</i>	7.0	5.0	45.6	46.8	144.2	262.1
<i>1994</i>	33.7	3.1	14.2	74.9	150.8	202.8
<i>1995</i>	9.0	4.2	31.3	178.4	204.3	202.7
<i>1996</i>	30.1	7.6	22.2	208.3	253.3	232.8
<i>1997</i>	7.6	39.1	17.5	72.3	174.1	208.0
<i>1998</i>	0.0	0.8	11.8	5.6	165.5	171.2
<i>1999</i>	11.6	26.9	1.7	104.7	156.2	305.3
<i>2000</i>	4.3	0.0	6.4	8.5	156.7	305.8
<i>2001</i>	10.3	5.8	2.3	42.7	171.9	112.8
<i>2002</i>	0.0	0.0	0.0	0.0	0.0	228.8
<i>2003</i>	7.7	6.0	38.7	25.7	81.5	209.9
AVG	10.56	8.99	17.30	73.19	157.67	226.69

Todos Santos - Average monthly precipitation totals (mm)

	JUL	AUG	SEP	OCT	NOV	DEC
1990	179.9	73.8	275.7	75.4	145.1	85.0
1991	64.0	96.0	212.3	105.3	38.2	77.6
1992	94.6	104.3	149.4	36.5	55.1	11.8
1993	93.8	148.3	168.1	119.7	11.5	8.0
1994	90.4	150.2	129.9	75.6	22.4	9.3
1995	149.2	191.4	235.6	107.7	21.7	38.7
1996	293.4	199.2	160.8	186.0	163.9	22.9
1997	151.5	111.7	276.7	88.6	59.2	33.9
1998	126.2	93.3	165.1	97.8	91.5	8.9
1999	182.5	187.1	267.9	122.1	71.0	34.1
2000	72.1	247.4	401.7	124.2	40.8	10.9
2001	218.8	189.7	237.3	216.0	14.8	0.7
2002	125.9	88.2	241.6	90.6	36.3	27.2
2003	95.5	85.1	133.3	86.0	57.4	30.6
AVG	138.41	140.41	216.91	109.39	59.21	30.02

Todos Santos - Average monthly Humidity (%) (1990 - 2003)

	JAN	FEB	MAR	APR	MAY	JUN
AVG	83	80	80	81	85	86
	JUL	AUG	SEP	OCT	NOV	DEC
AVG	86	85	88	87	85	83

Todos Santos - Average monthly windpseed (km/hr) (1990 - 2003)

	JAN	FEB	MAR	APR	MAY	JUN
AVG	1.9	2.9	3.0	3.8	3.4	3.4
	JUL	AUG	SEP	OCT	NOV	DEC
AVG	3.5	3.7	3.2	4.2	4.0	4.9

Todos Santos - Average monthly cluodiness (1990 - 2003)

	JAN	FEB	MAR	APR	MAY	JUN
AVG	46%	38%	36%	50%	71%	74%
	JUL	AUG	SEP	OCT	NOV	DEC
AVG	71%	70%	73%	71%	63%	59%

San Jose - Average mmonthly temperature (C)

	JAN	FEB	MAR	APR	MAY	JUN
<i>1990</i>	26.4	27.9	28.3	28.9	28.1	27.9
<i>1991</i>	24.9	25.4	26.8	28.0	28.6	27.7
<i>1992</i>	26.3	26.4	28.0	28.7	29.0	28.4
<i>1993</i>	25.8	26.1	27.7	29.1	28.8	27.8
<i>1994</i>	25.3	26.8	27.7	28.8	29.0	28.1
<i>1995</i>	26.0	27.0	27.5	27.1	28.9	28.1
<i>1996</i>	25.3	26.3	27.0	28.3	27.8	28.0
<i>1997</i>	26.0	26.9	28.4	28.4	29.1	28.0
<i>1998</i>	26.9	26.6	28.5	29.0	29.2	nd
<i>1999</i>	26.2	26.3	27.5	28.2	28.5	27.8
<i>2000</i>	23.7	25.8	27.2	28.6	27.9	28.3
<i>2001</i>	25.2	27.3	27.4	29.2	29.1	28.4
<i>2002</i>	26.4	27.1	28.1	29.5	29.4	28.3
<i>2003</i>	26.9	27.4	nd	29.4	28.9	28.0
AVG	25.81	26.66	27.70	28.66	28.74	28.06

San Jose - Average mmonthly temperature (C)

	JUL	AUG	SEP	OCT	NOV	DEC
<i>1990</i>	27.0	26.9	26.6	26.3	26.1	25.3
<i>1991</i>	27.9	27.4	27.6	27.5	26.7	25.8
<i>1992</i>	27.4	27.9	26.9	27.5	27.1	26.7
<i>1993</i>	28.3	27.8	27.1	27.4	26.7	26.0
<i>1994</i>	28.5	28.0	27.6	27.1	27.0	27.4
<i>1995</i>	27.7	27.3	27.2	26.8	27.3	26.6
<i>1996</i>	27.4	27.4	27.5	27.2	26.8	25.7
<i>1997</i>	nd	28.5	27.5	26.5	27.4	27.0
<i>1998</i>	27.9	28.0	28.0	27.2	27.0	26.1
<i>1999</i>	27.6	27.6	26.3	26.2	25.9	25.2
<i>2000</i>	23.3	28.1	27.3	27.0	27.5	26.3
<i>2001</i>	28.4	28.7	27.3	27.7	27.0	26.7
<i>2002</i>	28.9	28.6	27.6	28.0	27.3	27.0
<i>2003</i>	nd	nd	nd	nd	nd	nd
AVG	27.5	27.9	27.3	27.1	26.9	26.3

San Jose - Average monthly precipitation totals (mm)

	JAN	FEB	MAR	APR	MAY	JUN
<i>1990</i>	0.0	38.0	0.0	105.4	329.7	307.3
<i>1991</i>	0.0	0.0	5.2	18.6	98.8	437.0
<i>1992</i>	0.0	0.0	83.1	53.0	123.9	266.1
<i>1993</i>	14.8	0.0	5.4	13.8	143.3	497.7
<i>1994</i>	0.0	0.0	0.0	30.5	103.9	149.8
<i>1995</i>	0.0	0.0	0.0	18.6	96.8	323.4
<i>1996</i>	4.8	0.0	0.0	69.6	167.7	419.0
<i>1997</i>	0.0	0.0	14.4	97.2	94.0	281.0
<i>1998</i>	0.0	0.0	0.0	0.0	40.0	263.3
<i>1999</i>	0.0	0.0	14.0	59.4	108.6	434.9
<i>2000</i>	0.0	0.0	32.0	18.7	353.8	181.3
<i>2001</i>	0.0	0.0	10.5	1.6	114.8	190.2
<i>2002</i>	0.0	0.0	0.0	3.1	268.1	208.7
<i>2003</i>	0.0	0.0	0.0	66.0	159.6	547.2
AVG	1.40	2.71	11.76	39.68	157.36	321.92

San Jose - Average monthly precipitation totals (mm)

	JUL	AUG	SEP	OCT	NOV	DEC
<i>1990</i>	216.3	163.5	107.0	263.6	46.1	29.6
<i>1991</i>	210.0	175.7	150.2	97.8	37.2	7.6
<i>1992</i>	434.1	160.3	419.5	94.8	77.9	0.0
<i>1993</i>	332.7	245.0	374.2	90.8	25.7	0.0
<i>1994</i>	98.5	330.8	203.4	197.1	45.4	13.0
<i>1995</i>	138.3	472.1	176.2	271.3	10.8	3.6
<i>1996</i>	nd	366.1	292.9	167.6	72.8	0.0
<i>1997</i>	285.8	136.8	636.9	363.2	185.9	41.2
<i>1998</i>	414.4	323.8	221.5	446.0	946.0	0.0
<i>1999</i>	396.0	183.8	517.5	205.6	nd	nd
<i>2000</i>	119.8	164.5	276.7	225.9	73.3	0.0
<i>2001</i>	318.5	56.4	296.9	89.4	15.7	0.0
<i>2002</i>	170.1	148.0	237.9	123.1	8.6	0.0
<i>2003</i>	nd	nd	nd	nd	nd	nd
AVG	261.21	225.14	300.83	202.78	128.78	7.92

APPENDIX II

GUATEMALAN TEMPERATURE AND PRECIPITATION

Table of climate data showing yearly averages for 64 stations throughout Guatemala; given is the altitude above sea level (a.s.l.), average annual precipitation totals and average annual temperature for each station. Since this data presented only one annual average it could not be used for the Plummer and Phillips, (2003) model which required monthly and even daily climate input.

Location (Guatemala)	a.s.l. (m)	Average annual Precipitation totals (mm)	Average annual Temperature (°C)
Puerto Barrios	0	3111.3	27.6
Livingston	10	1825.6	26.0
Moyuta	10	1389.4	26.8
San Luis	10	4125.8	25.7
Panzos	30	2656.7	26.6
San Andres	60	1633.2	26.3
Tiquisate	70	2016	27.7

Los Amates	76	1800.3	27.1
Panzos, papalha	120	1911.4	26.0
Flores	123	1553.1	25.7
Libertad	125	1843.8	25.5
Chisec	140	2477.5	25.8
Retalhuleu	205	2890.7	27.4
Estanzuela	210	652.3	27.7
Catarina	233	3565.4	26.0
Rio Hondo	260	721.3	26.9
Escuintla, El chupadero	270	2755.3	27.3
Sta. Lucia Cotz. Camantulul	280	3516.1	25.5
El Asintal	355	3010.6	25.5
Morazan	370	780.5	27.0
Cahabon	380	2386.3	25.3
Mazatenango	430	3527.3	24.8
Camotan	450	963.7	25.8
Asunción Mita	478	1241.3	27.1
Poptun	500	1849.1	23.4
San Juan Bautista	670	3204.3	24.6
Chicaman	680	1238.1	24.3
Escuintla	730	3124.8	23.8
Cuilapa	737	1552.3	23.8
Ipala	828	920.1	23.7

La Union	885	1592.1	21.9
Cubulco	944	903.3	21.7
Esquipulas	950	1551.6	22.3
Monjas	960	974.6	22.0
Quezada	980	1104.1	22.4
Sn. Jeronimo	1000	908.6	21.6
Villa Canales	1120	1523.9	22.6
Cuilco	1120	985.2	22.8
Sacapulas	1180	834.1	21.7
Amatitlan	1189	924	21.0
San Pedro Ayampuc	1200	1063.1	21.4
Sn. Migel Petapa.	1260	1093.7	21.4
Coban	1323	2074.9	18.8
San Pedro Sacatepequez	1400	1031.9	19.9
Guatemala, Florinda	1470	1310.3	20.6
Guatemala, INSIVUMEH	1502	1196.8	19.3
San Lucas Toliman	1562	1011.7	19.9
Santiago Atitlan	1580	1010	18.4
San José Pinula	1650	1639.3	17.3
San Pedro Necta	1700	1475.3	19.0
Jalapa	1760	1002.8	15.2
Sn. Martin Jilotepeque	1800	1272.7	17.8
Santa Lucia la Reforma	1840	938.7	18.6

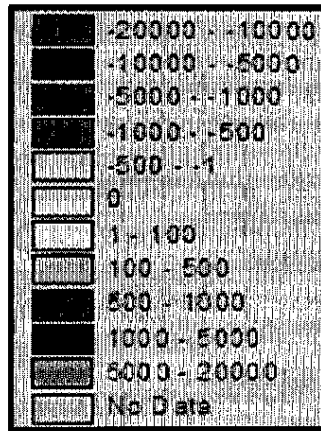
Huehuetenango	1870	974.9	17.7
Chinique	1880	1543.9	16.6
Nebaj	1906	1925.6	15.9
Chichicastenango	2025	1386.4	15.8
Santa Maria de Jesus	2065	1221.1	16.1
Santa Cruz Balanya	2080	970.4	16.1
San Lucas Sacatepequez	2105	991.8	12.7
San Pedro Soloma	2260	2138.8	13.4
Olintepeque	2380	842.5	13.8
San Marcos	2420	1026.5	13.0
Todos los Santos	2480	1155	14.2

APPENDIX III

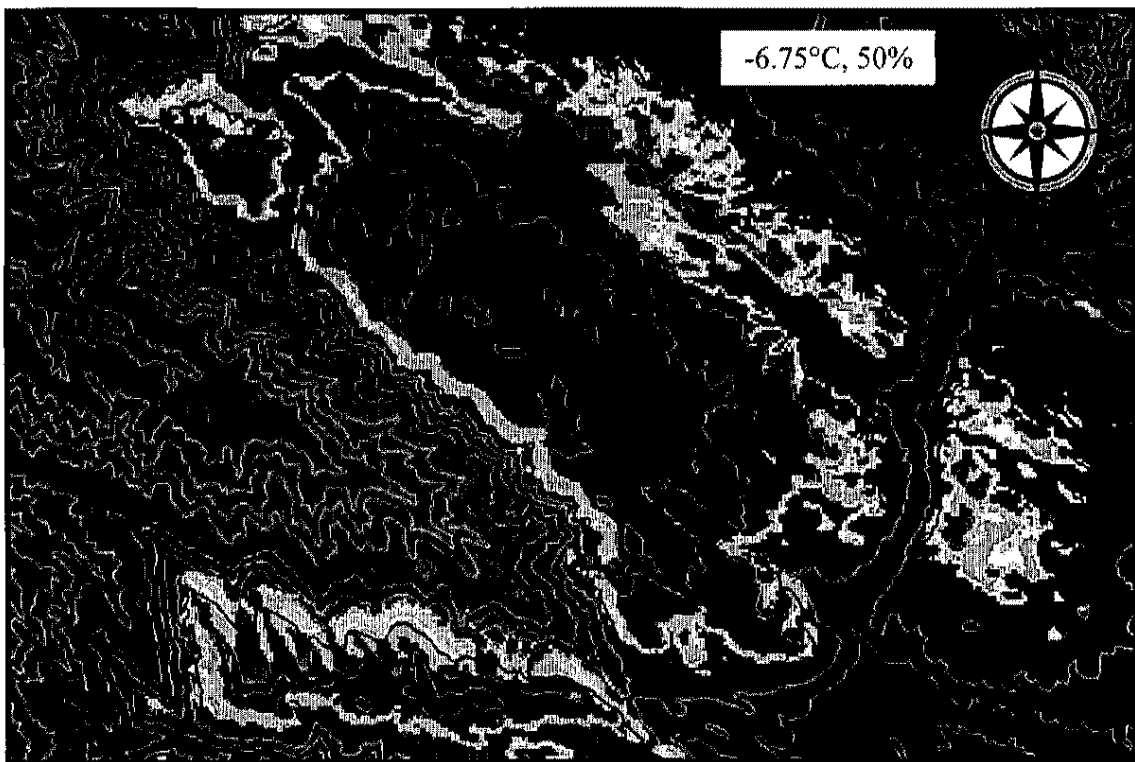
EXAMPLES OF MASS BALANCE MODEL OUTPUT

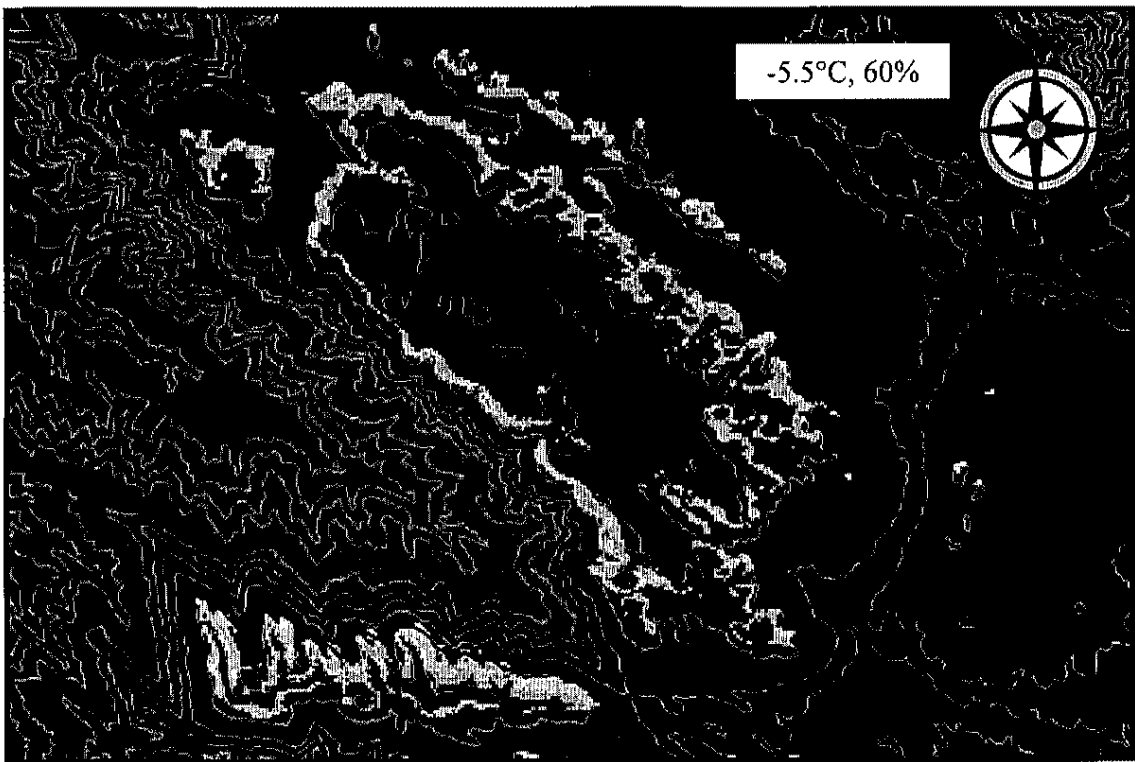
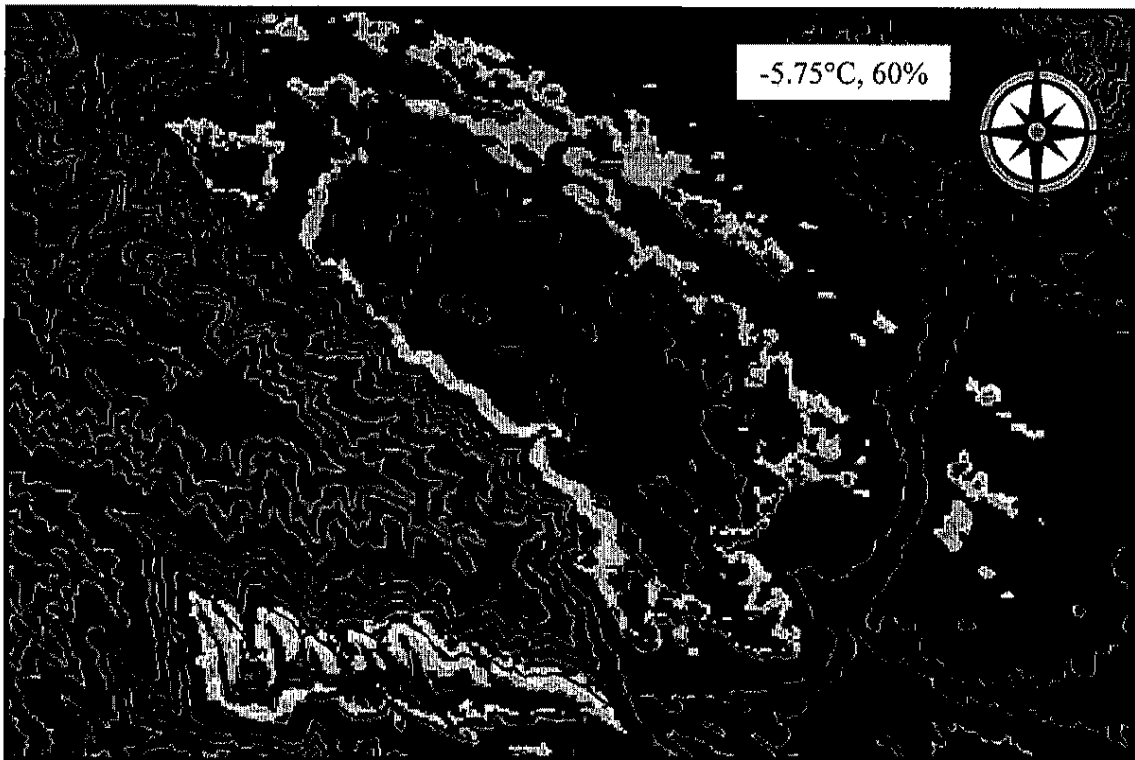
Selected output maps of the Plummer and Phillips, (2003) mass balance GIS model, scale bar is 1m, mass balance scale can be found in figure 10. Present are only 10 out ~50 iterations completed for this research, although these represent model outputs that demonstrate the sensitivity of the model results. Modeled areas of 0 mass balance that matched the target ELAs of the plateau region (3650 m) and Montaña San Juan (3500 m) were used to determine the northern Guatemalan highlands paleoclimate. Each map has the corresponding temperature depression (°C) and the % of present day precipitation given in white lettering.

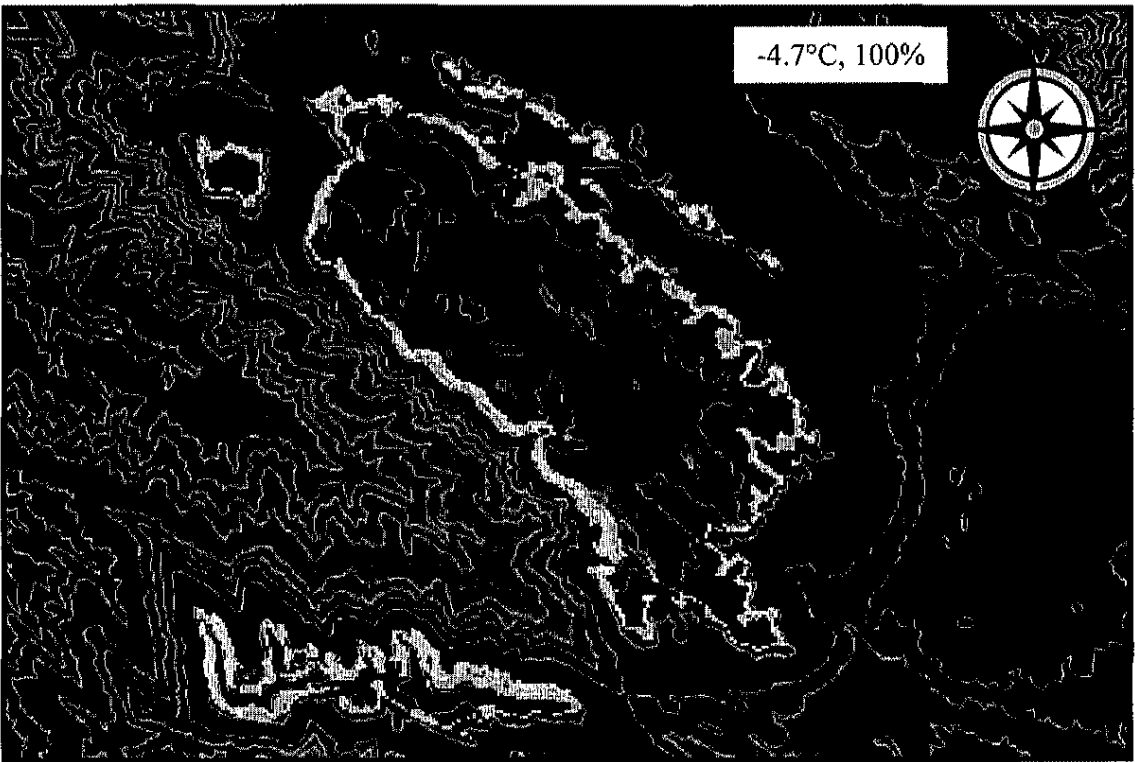
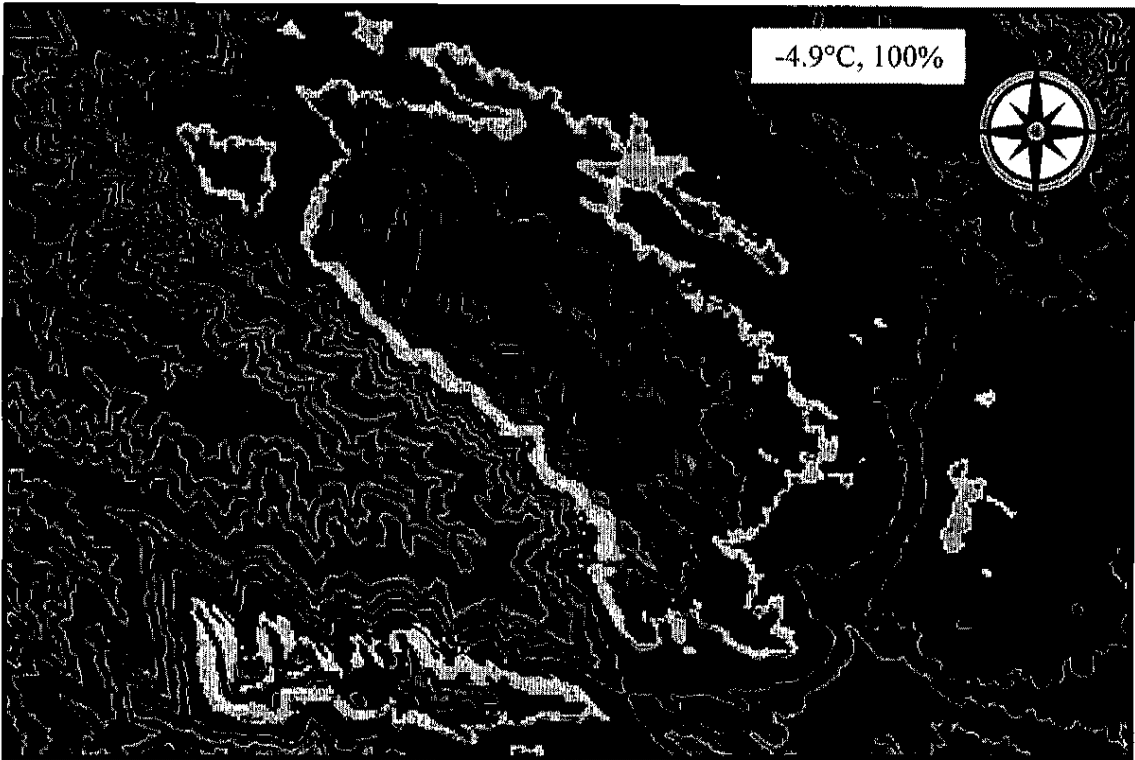
The mass balance output of the plateau and Montaña San Juan region is shown by areas of net annual accumulation (blue to purple) and net annual ablation (reds to green). The ELA was estimated from grids on the output data that were equal to 0 mm of net annual accumulation/ablation. The scale used in the GIS model is given below, measured in mm water equivalent of the net annual accumulation and ablation for the modeled region.

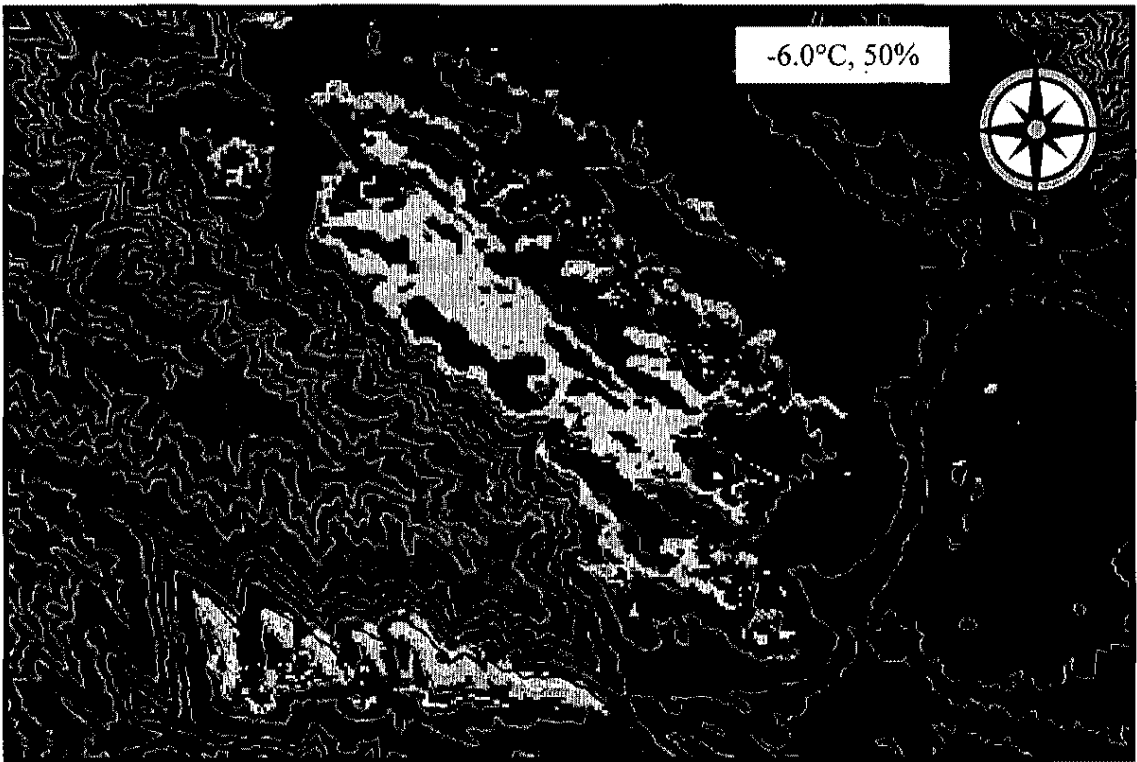
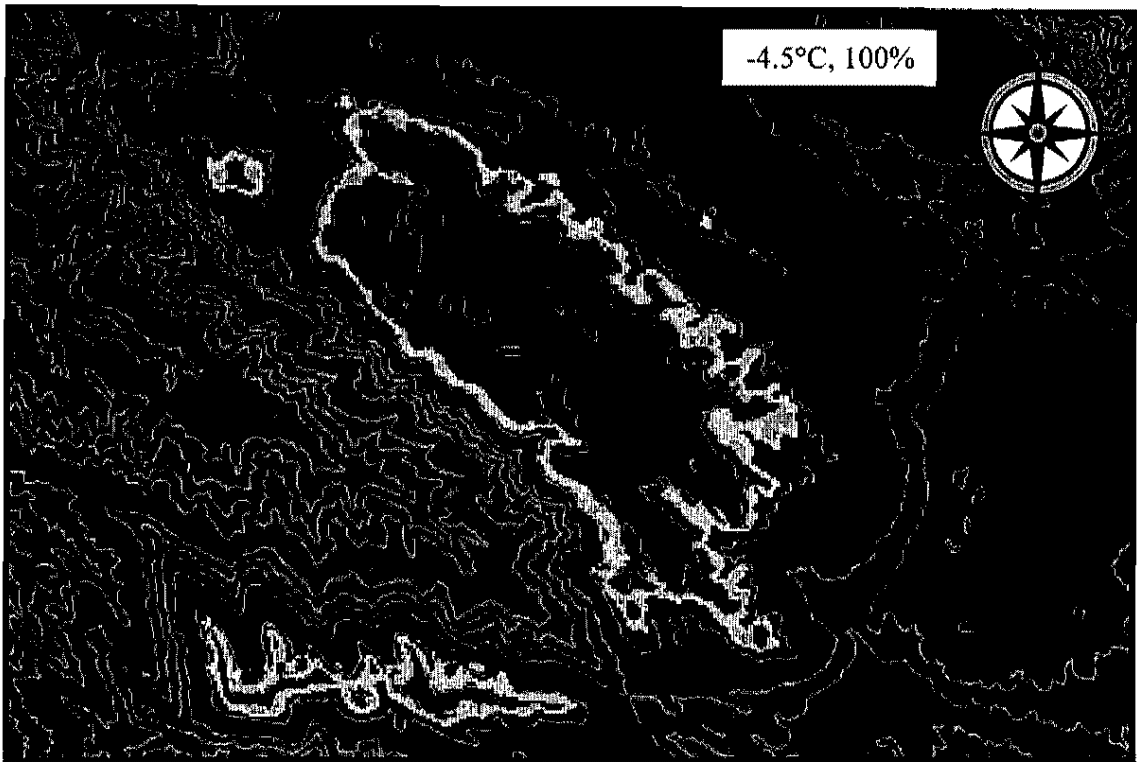


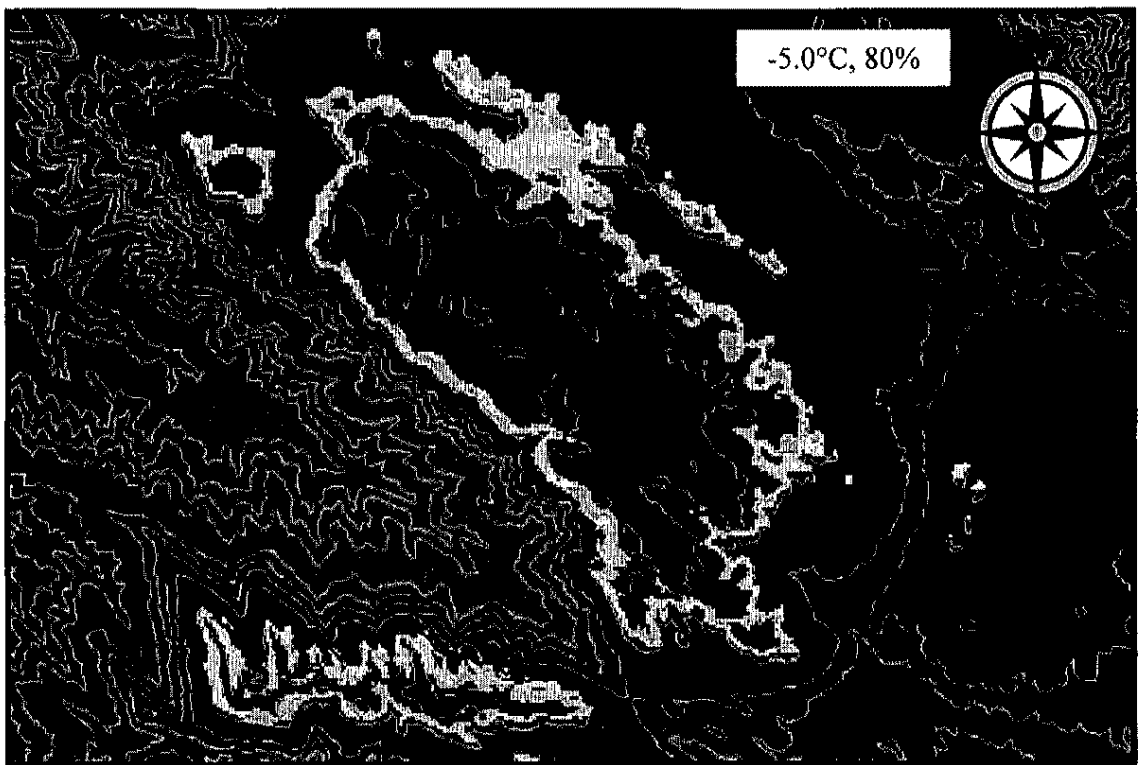
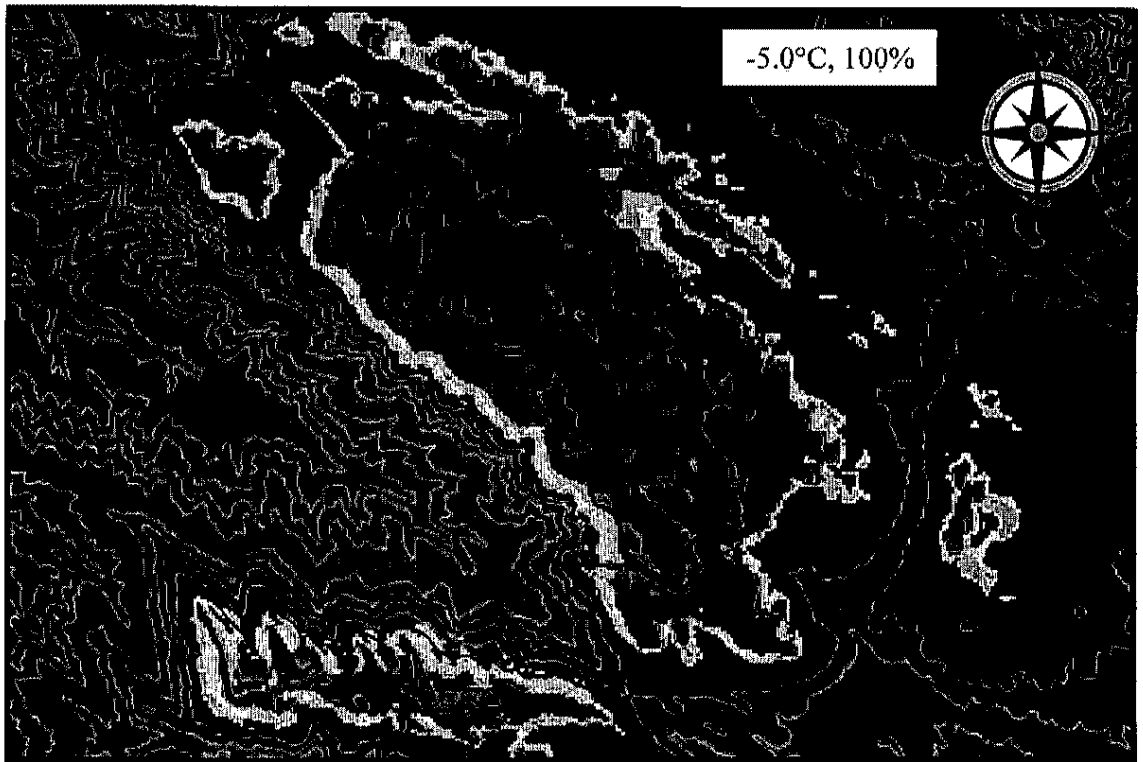
Key represents mm water equivalent











VITA

Graduate College
University of Nevada, Las Vegas

Alex J. Roy

Local Address:

2455 Paradise Village Way
Las Vegas, NV 89120

Home Address:

16475 Harms Way
Piney Point, MD 20674

Degrees:

Bachelor of Science, Earth Science, 2005
University of Maine

Awards and Scholarships:

Bernada E. French Scholarship in Geology, UNLV, 2007
Graduate and Professional Student Association Grant, UNLV, 2005; 2006
National Science Foundation, Research for Undergraduates Grant, UM, 2002

Thesis Title:

The Mayan Ice Cap: Glacial Geology and Paleoclimate of the Northern Guatemalan Highlands

Thesis Examination Committee:

Chairperson, Dr. Matthew Lachniet, Ph.D.
Committee Member, Dr. Andrew Hanson, Ph.D.
Committee Member, Dr. Terry Spell, Ph.D.
Graduate Faculty Representative, Dr. John Swetnam, Ph.D.